

Responses to Comments from Reviewer and Editor

Thanks for the comments and suggestions. The point-by-point response is given below, in bold.

The discussion section could be moved earlier in the paper (before the conclusions section) - this would be a more usual structure and would help give the conclusions more prominence.

R: Agree, it is moved.

Following my previous comment on calculating the CDNC, the gridbox mean values are not really suitable for calculating the CDNC as the calculation is highly non-linear. Doing the calculation using the joint histogram does not require that much more work, but will produce better results. This may not change the results much, but it might be a good idea for future studies at the very least. I have attached a plot of the mean CDNC in March-April-May over the study region, calculated from the MODIS L3 histograms for the period 2006-2010 (the data I had easily available). The plot on the left shows the mean CDNC across the nearby region.

R: Thanks. We very much appreciate the illustrated plot. We have followed the suggestion using the joint histogram data; see Section 2.1.3 and all the CDNC values and relevant tables/figures have been changed. As pointed out by the Reviewer, the main conclusions remain.

The English in the paper could still use some improvement, although the meaning is usually clear. I have not gone through the paper again to highlight all the changes, but they seem to be primarily in the new sections.

R: We have polished the manuscript.

Other comments:

L307 - The SH is defined correctly earlier as the specific humidity, rather than the "water vapor content"

R: The sentence is deleted.

L434 - The cases of heavy rainfall using CDNC seem more extreme - then at L440 - the change in rainfall intensity is not significant. Please clarify this

R: The "extreme" did not mean the rainfall intensity, but the bigger difference between clean and polluted cases using CDNC. Since we re-calculated the CDNC, and accordingly this sentence is now meaningless and has been deleted.

L639 - 'accumulate more water in the cloud' - Is this a reference to some kind of Albrecht (1989) type effect? If so, it might be good to state it (although an earlier start to precipitation does not match this). If not, it would also be good to state it (and explain what it is).

R: Our results indicate that the CF, COT and CWP become larger when AOD/CDNC increases (Sect. 4.1) and that the liquid CER becomes larger when moisture increases in the polluted environment (Sect. 4.2), we suggest that more aerosols can serve as CCN, which in a moisture sufficient environment can hold more liquid water in the cloud. Therefore, it is not the same as the second indirect effect on cloud extent and lifetime as in Albrecht (1989), which states that, for a fixed liquid water path, the increased CCN would lead to smaller cloud particle sizes and thus suppression of precipitation and prolonging of the cloud lifetime. The sentence is modified accordingly, see L410-412 and L468-470.

L654(and associated section) - CDNC is not CCN. As the editor has pointed out, in an updraft limited regime, variations in CDNC come primarily from changes in updraft. Just stating that you are using CDNC to represent CCN does not make CDNC actually represent CCN.

R: Yes, it is re-written, see L427 and L432.

L694 - Following from my comments in previous reviews - The relationship is not completely meaningless, just difficult to interpret. Also, this sentence does not make much sense to me - you state that this comparison cannot be done, then use it to infer the role of aerosols. I would suggest you leave this sentence out, you have plenty of other results without relying on this.

R: Agree, the sentence is deleted.

L853 - It is not clear the large scale updraft is a good measure of the in-cloud updraft relevant for droplet formation.

R: Agree, we have modified the statement, see L550-553.

1 **An observational study of the effects of aerosols on diurnal variation of heavy rainfall**
2 **and associated clouds over Beijing-Tianjin-Hebei**

3
4 Siyuan Zhou^{1,2,3}, Jing Yang^{1,2*}, Wei-Chyung Wang³, Chuanfeng Zhao⁴, Daoyi Gong^{1,2}, Peijun Shi^{1,2}

5
6 ¹ State Key Laboratory of Earth Surface Process and Resource Ecology, Beijing Normal University, China

7 ² Key Laboratory of Environmental Change and Natural Disaster, Faculty of Geographical Science, Beijing
8 Normal University, China

9 ³ Atmospheric Sciences Research Center, State University of New York, Albany, New York 12203, USA

10 ⁴ College of Global Change and Earth System Science, Beijing Normal University, China

11
12
13 Submitted to ACP

14 Oct 2018

15
16
17
18
19
20
21
22
23
24
25
26
27
28
29
30
31
32
33 *Correspondence to: Jing Yang, State Key Laboratory of Earth Surface Process and Resource Ecology/ Key
34 Laboratory of Environmental Change and Natural Disaster, Faculty of Geographical Science, Beijing Normal
35 University, 19#Xinjiekouwai Street, Haidian District, Beijing 100875, China. E-mail: yangjing@bnu.edu.cn

36 **Abstract:** Our previous study found that the observed rainfall diurnal variation over Beijing-Tianjin-Hebei
37 shows distinct signature of the effects of pollutants. Here we used the hourly rainfall data together with
38 satellite-based daily information of aerosols and clouds to further investigate changes in heavy rainfall and
39 clouds associated with aerosol changes. Because of the strong coupling effects, we also examined the
40 sensitivity of these changes to moisture (specific humidity) variations. For heavy rainfall, three distinguished
41 characteristics are identified: *earlier start time*, *earlier peak time*, and *longer duration*; and the signals are
42 robust using aerosol indicators based on both aerosol optical depth and cloud droplet number concentration.
43 In-depth analysis reveals that the first two characteristics occur in the presence of (absorbing) black carbon
44 aerosols and that the third is related to more (scattering) sulfate aerosols and sensitive to moisture abundance.
45 Cloud changes are also evident, showing increases in cloud fraction, cloud top pressure, the liquid/ice cloud
46 optical thickness and cloud water path, and decrease in ice cloud effective radius; and these changes are
47 insensitive to moisture. Finally, the mechanisms for heavy rainfall characteristics are discussed and
48 hypothesized.

49 **Key words: aerosol, heavy rainfall, diurnal variation, cloud, Beijing-Tianjin-Hebei, observational study**

50

51 **1. Introduction**

52 Aerosols modify the hydrologic cycle through direct radiative and indirect cloud adjustment effects (IPCC,
53 2013). The direct effect, through absorbing and scattering solar radiation, leads to heating in the atmosphere
54 (e.g. Jacobson 2001; Lau et al. 2006) and cooling on the surface (Lelieveld and Heintzenberg 1992; Guo et al.
55 2013; Yang et al., 2018), causing changes in atmospheric vertical static stability and subsequently modulation
56 of rainfall (e.g. Rosenfeld et al. 2008). On the other hand, water-soluble aerosols serving as cloud
57 condensation nuclei (CCN) affect the warm-rain and cold-rain processes through influencing the cloud droplet
58 size distributions, cloud top heights and other cloud properties (Jiang et al., 2002; Givati and Rosenfeld 2004;
59 Chen et al., 2011; Lim and Hong 2012; Tao et al., 2012). For Beijing-Tianjin-Hebei (BTH) the significant
60 increase in pollution in recent decades has raised issues concerning aerosol-radiation-cloud-precipitation
61 interactions. While the impact of aerosols on light rainfall or warm-rain processes is in general agreement
62 among studies for this region (e.g., Qian et al., 2009), the uncertainties of the effects on heavy convective
63 rainfall are still large (Guo et al., 2014; Wang et al., 2016).

64 The clouds that can generate heavy convective rainfall in BTH region usually contain warm clouds, cold
65 clouds and mixed-phase clouds (e.g. Guo et al., 2015). Because the aerosol-cloud interactions in different
66 types of clouds are distinct (Gryspeerd et al., 2014b), aerosol indirect effect during heavy rainfall is more
67 complicated than its direct effect (Sassen et al., 1995; Sherwood, 2002; Jiang et al., 2008, Tao et al., 2012).
68 For warm clouds, by serving as CCN that nucleates more cloud droplets, aerosols can increase cloud albedo so
69 called albedo effect or Twomey effect (Twomey, 1977), lengthen the cloud lifetime so called lifetime effect

70 (Albrecht, 1989), and enhance thin cloud thermal emissivity so called thermal emissivity effect (Garrett and
71 Zhao, 2006). The above effects tend to increase the cloud microphysical stability and suppress warm-rain
72 processes (Albrecht 1989; Rosenfeld et al. 2014). For cold clouds and mixed-phase clouds, many studies
73 reported that the cloud liquid accumulated by aerosols is converted to ice hydrometeors above the freezing
74 level, which invigorates deep convective clouds and intensifies heavy precipitation so called invigoration
75 effect (Rosenfeld and Woodley, 2000; Rosenfeld et al., 2008; Lee et al. 2009; Guo et al. 2014). The Twomey
76 effect infers that aerosols serving as CCN that increase the cloud droplets could reduce cloud droplet size
77 within a constant liquid water path (Twomey, 1977). However, the opposite results of relationship between
78 aerosols and cloud droplet effective radius were reported in observations (Yuan et al., 2008; Panicker et al.,
79 2010; Jung et al., 2013; Harikishan et al., 2016; Qiu et al., 2017), which might be related with the moisture
80 supply near the cloud base (Yuan et al., 2008; Qiu et al., 2017). Besides, the influence of aerosols on ice
81 clouds also depends upon the amount of moisture supply (Jiang et al., 2008). Therefore, how the aerosols
82 modify the heavy convective rainfall and associated cloud changes does not reach a consensus, particularly if
83 considering the different moisture conditions.

84 Heavy convective rainfall over BTH region usually occurs within a few hours, thus studying on the
85 relationship between aerosols and rainfall diurnal variation could deepen our understanding of aerosol effects
86 on heavy rainfall. Several previous studies have found that aerosols are related to the changes of the rainfall
87 diurnal variation in other regions (Kim et al., 2010; Gryspeerd et al., 2014b; Fan et al., 2015; Guo et al., 2016;
88 Lee et al., 2016). However, the above studies do not address the change of cloud properties and its sensitivity
89 to different conditions of moisture supply. Although our recent work over BTH region (Zhou et al. 2018)
90 attempted to remove the meteorological effect including circulation and moisture and found that the peak of
91 heavy rainfall shifts earlier on the polluted condition, it only excluded the extreme moisture conditions and
92 focused on aerosol radiative effect on the rainfall diurnal variation. Therefore, this study aims to deepen the
93 previous study (Zhou et al., 2018) through investigating the following questions: (1) how do aerosols
94 (including absorbing aerosols and scattering aerosols) modify the behaviors of the heavy rainfall diurnal
95 variation (start time, peak time, duration and intensity)? And what is the role of moisture in them? (2) how do
96 aerosols influence the associated cloud properties with inclusion of moisture? To solve above questions, we
97 used aerosol optical depth (AOD) as a macro indicator of aerosol pollution and cloud droplet number
98 concentration (CDNC) as a micro indicator of CCN served by aerosols respectively to compare the
99 characteristics of heavy rainfall diurnal variation and associated cloud properties between clean and polluted
100 conditions, and applied aerosol index (AI) to distinguish the different effects of absorbing aerosols and
101 scattering aerosols. In addition, we used the specific humidity (SH) at 850 hPa as an indicator of moisture
102 condition to investigate the possible role of moisture in the relationship between aerosols and rainfall or
103 clouds. The paper is organized as following: The data and methodology are introduced in Sect. 2. Section 3
104 addresses the relationship between aerosol pollution and diurnal variation of heavy rainfall, covering the
105 distinct characteristics of heavy rainfall on clean/polluted condition; the different behaviors of heavy rainfall

- Siyuan 20/2/19 11:34 PM
已删除: associated
- Siyuan 20/2/19 11:34 PM
已删除: supply
- Siyuan 20/2/19 11:34 PM
已删除: effects
- Siyuan 20/2/19 11:34 PM
已删除: on
- Siyuan 20/2/19 11:34 PM
已删除: and
- Siyuan 20/2/19 11:34 PM
已删除: and compared them with the effects of aerosols
- Siyuan 20/2/19 11:34 PM
已删除: using AOD and CDNC

114 diurnal variation along with different types of aerosols, and the influence of moisture on the relationship
115 between aerosols and heavy rainfall. Section 4 describes the concurrent changes of cloud properties associated
116 with aerosols and compares the possible influences of CCN (represented by CDNC) and moisture (represented
117 by SH) on the cloud properties. Section 5 gives the hypothesis about the mechanisms of aerosol effects on the
118 heavy rainfall. Discussion and conclusions will be given in Sect. 6.

119

120 2. Approach

121 2.1 Data

122 Four types of datasets from the year 2002 to 2012 (11 years) are used in this study, which include (1)
123 precipitation, (2) aerosols, (3) clouds, and (4) other meteorological fields.

124 2.1.1 Precipitation

125 To study the diurnal variation of heavy rainfall, the gauge-based hourly precipitation datasets are used, which
126 were obtained from the National Meteorological Information Center (NMIC) of the China Meteorological
127 Administration (CMA) (Yu et al., 2007) at 2420 stations in China from 1951 to 2012. The quality control
128 made by CMA/NMIC includes the check for extreme values (the value exceeding the monthly maximum in
129 daily precipitation was rejected), the internal consistency check (wiping off the erroneous records caused by
130 incorrect units, reading, or coding) and spatial consistency check (comparing the time series of hourly
131 precipitation with nearby stations) [Shen et al., 2010]. Here we chose 176 stations in the plain area of BTH
132 region that are below the topography of 100 meter above sea level as shown in Fig.1, because we purposely
133 removed the probable orographic influence on the rainfall diurnal variation, which is consistent with our
134 previous work (Zhou et al., 2018). The record analyzed here is the period of 2002 to 2012. We selected heavy
135 rainfall days when the hourly precipitation amount is more than 8.0 mm/hour (defined by *Atmospheric*
136 *Sciences Thesaurus, 1994*). Here “a day” is counted from 8 LST to 8 LST next day (0 UTC to 24 UTC).

137 2.1.2 Aerosols

138 In this study, we used two satellite data and one reanalysis data to investigate the aerosol optical amount and
139 distinguish the different aerosol types.

140 AOD is a proxy for the optical amount of aerosol particles in a column of the atmosphere and serves as the
141 macro indicator for the division of aerosol pollution condition in this study, which was obtained from MODIS
142 (Moderate Resolution Imaging Spectroradiometer) Collection 6 Level-3 aerosol product with the horizontal
143 resolution of 1°x1° onboard the Terra satellite (Tao et al., 2015). The quality assurance of marginal or higher
144 confidence is used in this study. The reported uncertainty in MODIS AOD data is on the order of (-0.02-10%),
145 (+0.04+10%) (Levy et al., 2013). The Terra satellite overpass time at the equator is around 10:30 local solar
146 time (LST) in the daytime, and the satellite data is almost missing when it is rainy during the overpass time.

Siyuan 20/2/19 11:34 PM

已删除: comparison

Siyuan 20/2/19 11:34 PM

已删除: heavy rainfall behaviors influenced respectively by

Siyuan 20/2/19 11:34 PM

已删除: and

Siyuan 20/2/19 11:34 PM

已删除: (CCN

Siyuan 20/2/19 11:34 PM

已删除: Conclusions

Siyuan 20/2/19 11:34 PM

已删除: discussion

Siyuan 20/2/19 11:34 PM

已删除: L3

155 As shown in Fig.3, the occurrence of selected heavy rainfall events in this study is mainly later than the
156 satellite overpass time. Therefore, the AOD used here represents the situation of the air quality in advance of
157 heavy rainfall appearance. Many studies have indicated the value of AOD is influenced by moisture condition,
158 which is aerosol humidification effect (Twohy et al., 2009; Altaratz et al., 2013). Hence, we comprehensively
159 analyzed the moisture effect on the rainfall and tried to remove the moisture effect from the relationship
160 between aerosols and rainfall/clouds.

161 The ultraviolet AI from Ozone Monitoring Instrument (OMI) on board the Aura satellite which was
162 launched in July 2004, is used for detecting the different types of aerosols in this study. The OMI ultraviolet
163 AI is a method of detecting absorbing aerosols from satellite measurements in the near-ultraviolet wavelength
164 region (Torres et al., 1998). The positive values of ultraviolet AI are attributed to the absorbing aerosols such
165 as smoke and dust while the negative values of AI stand for the non-absorbing aerosols (scattering aerosols)
166 such as sulfate and sea salt (Tariq and Ali, 2015). The near-zero values of AI occur when clouds and Rayleigh
167 scattering dominate (Hammer et al., 2018). Considering the near-zero values have more uncertainties, we only
168 compare the extreme circumstances of absorbing aerosols and scattering aerosols in this study. The horizontal
169 resolution of AI data is $1^{\circ} \times 1^{\circ}$ and it covers the period of 2005 to 2012.

170 MACC-II (Monitoring Atmospheric Composition and Climate Interim Implementation) reanalysis product
171 produced by ECMWF (the European Centre for Medium-Range Weather Forecasts), provided the AOD
172 datasets for different kinds of aerosols (BC, sulfate, organic matter, mineral dust and sea salt). MACC-II
173 reanalysis products are observationally-based within a model framework, which can offer a more complete
174 temporal and spatial coverage than observation and reduce the shortcomings of simulation that fail in
175 simulating the complexity of real aerosol distributions (Benedetti *et al.*, 2009). The horizontal resolution of
176 MACC-II is also $1^{\circ} \times 1^{\circ}$ with the time interval of six-hour covering the period of 2003 to 2012, and the daily
177 mean values are used in this study in order to be consistent with other datasets.

178 2.1.3 Clouds

179 Daily cloud variables, including cloud fraction (CF), cloud top pressure (CTP), cloud optical thickness (COT,
180 liquid and ice), cloud water path (CWP, liquid and ice) and cloud effective radius (CER, liquid and ice), were
181 obtained from MODIS Collection 6 Level-3 cloud product onboard the Terra satellite. The MODIS cloud
182 product combines infrared emission and solar reflectance techniques to determine both physical and radiative
183 cloud properties (Platnick et al., 2017). The validation of cloud top properties in this product has been
184 conducted through comparisons with CALIOP (Cloud-Aerosol Lidar with Orthogonal Polarization) data and
185 other lidar observations (Holz et al., 2008; Menzel et al., 2008), and the validation and quality control of cloud
186 optical products is performed primarily using in situ measurements obtained during field campaigns as well as
187 the MODIS Airborne Simulator instrument (<https://modis-atmos.gsfc.nasa.gov/products/cloud>). Consistent
188 with AOD, the measure of above cloud variables is before the occurrence of heavy rainfall.

Siyuan 20/2/19 11:34 PM
已删除: results in the analysis of heavy rainfall show consistent based on the

Siyuan 20/2/19 11:34 PM
已删除: which is shown in the figures and morning values that before the occurrence of heavy rainfall. MACC-II data covers the period of 2003 to 2012

Siyuan 20/2/19 11:34 PM
已删除: L3

196 In addition to the variables in MODIS cloud product, we also calculated CDNC using the [joint histogram of](#)
197 liquid COT and CER [from the MODIS Collection 6 Level-3 cloud](#) product. CDNC is retrieved as the proxy
198 for CCN and also the micro indicator for separating different aerosol conditions in this study. Currently, most
199 derivations of CDNC assume that the clouds are adiabatic and horizontally homogeneous; CDNC is constant
200 throughout the cloud's vertical extent, and cloud liquid water content varies linearly with altitude adiabatically
201 (Min et al., 2012; Bennartz and Rausch, 2017). According to Boers et al. (2006) and Bennartz (2007), we
202 calculated CDNC (unit: cm^{-3}) through:

$$203 \quad \text{CDNC} = \frac{C_w^{1/2}}{k} \frac{10^{1/2}}{4\pi\rho_w^{1/2}} \frac{\tau^{1/2}}{R_e^{5/2}} \quad (1)$$

204 Where C_w is the moist adiabatic condensate coefficient, and its value depends slightly on the temperature
205 of the cloud layer, ranging from 1 to $2.5 \times 10^{-3} \text{ gm}^{-4}$ for a temperature between 0 °C and 40 °C (Brennguier,
206 1991). In this study, we calculated the C_w through the function of the temperature (see Fig.1 in Zhu et al.,
207 2018) at a given pressure that is 850 hPa. And we have tested the sensitivity of CDNC to the amount of C_w
208 and found it almost keeps the same when the C_w changes from 1 to $2.5 \times 10^{-3} \text{ gm}^{-4}$. The coefficient k is the
209 ratio between the volume mean radius and the effective radius, and varies between 0.5 and 1 (Brennguier et al.,
210 2000). Here we used $k = 1$ for that we cannot get the accurate value of k and the value of k does not influence
211 the rank of CDNC for the division of aerosol condition in this study. ρ_w is cloud water density. τ and R_e are
212 the liquid COT and CER [with twelve and nine bins respectively in the joint histogram, and we calculated the](#)
213 [CDNC of each bin and get the grid mean CDNC based on the probability distribution of the bin counts from](#)
214 [the joint histogram](#). To reduce the uncertainty of CDNC retrieval caused by the heterogeneity effect from thin
215 clouds (Nakajima and King, 1990; Quaas et al., 2008; Grandey and Stier, 2010; Grosvenor et al., 2018), we
216 selected the CF more than 80%, the liquid COT more than 4 and the liquid CER more than $4 \mu\text{m}$ when
217 calculating the CDNC (Quaas et al., 2008).

218 2.1.4 Other meteorological data

219 In this study, wind, temperature, pressure and SH data, were obtained from the ERA-Interim reanalysis
220 datasets with $1^\circ \times 1^\circ$ horizontal resolution and 37 vertical levels at six-hour intervals. The daily mean values of
221 these variables are used in the study. ERA-Interim is a global atmospheric reanalysis produced by ECMWF,
222 which covers the period from 1979 to near-real time (Dee et al., 2011).

224 2.2 Methodology

225 We used both station data of gauge-based precipitation and gridded data including aerosols, clouds and other
226 meteorological variables. Gridded datasets in this study were downloaded with the horizontal resolution of
227 $1^\circ \times 1^\circ$, which are consistent with the resolution of MODIS [Level-3](#) products. To unify the datasets, we
228 interpolated all the gridded datasets onto the selected 176 rainfall stations using the average value in a $1^\circ \times 1^\circ$

Siyuan 20/2/19 11:34 PM

已删除: in this

Siyuan 20/2/19 11:34 PM

已设置格式: 下标

Siyuan 20/2/19 11:34 PM

已删除: obtained from MODIS Collection 6 L3 cloud product

Siyuan 20/2/19 11:34 PM

已设置格式

Siyuan 20/2/19 11:34 PM

已删除: resolution

Siyuan 20/2/19 11:34 PM

已设置格式

Siyuan 20/2/19 11:34 PM

已删除: $1^\circ \times 1^\circ$.

Siyuan 20/2/19 11:34 PM

已删除: , and we also verified the results based on the morning values that before the occurrence of heavy rainfall.

Siyuan 20/2/19 11:34 PM

已删除: The SH, which stands for the water vapor content, serves as the indicator of moisture supply condition in this study.

Siyuan 20/2/19 11:34 PM

已删除: L3

241 grid as the background condition of each rainfall station, i.e., the stations in the same $1^{\circ}\times 1^{\circ}$ grid have the same
242 aerosol, cloud and meteorological conditions.

243 2.2.1 Selection of sub-season and circulation

244 Consistent with our previous work, we focused on the early summer period (1 June to 20 July) which is before
245 the large-scale rainy season start, in order to remove the large-scale circulation influence and identify the effect
246 of aerosols on local convective precipitation because BTH rainfall during this period is mostly convective
247 rainfall (Yu et al., 2007) with heavy pollution (Zhou et al., 2018). And to unify the background atmospheric
248 circulation, we only selected the rainfall days with southwesterly flow, which is the dominant circulation
249 accounting for 40% of total circulation patterns over the BTH region during early summer (Zhou et al., 2018).

250 2.2.2 Classification of clean/polluted cases and moisture conditions

251 With the circulation of southwesterly, we used two indicators to distinguish the clean and polluted conditions
252 from macro and micro perspectives, which are AOD and CDNC. The 25th and 75th percentiles of AOD/CDNC
253 of the whole rainfall days are used as the thresholds of clean and polluted conditions, and the values are
254 shown in Tab.1. There are 514 cases of heavy rainfall on the polluted days and 406 cases of that on the clean
255 days when using AOD, and [805/812](#) cases on the polluted/clean condition when using CDNC (Fig. 3).

256 The absorbing aerosols are detected using the positive values of AI that is named as absorbing aerosol index
257 (AAI) here, and we can retrieve the scattering aerosol index (SAI) using the negative values of AI. AAI and
258 SAI are also divided into two groups using the threshold of 25th/75th percentile as shown in Tab.1. We used
259 AAI/SAI more than 75th percentile as the extreme circumstances of absorbing/scattering aerosols to compare
260 their impacts on the heavy rainfall. The sample numbers are 375 and 550 respectively for the extreme AAI
261 and SAI cases. Using the same method, we chose cases with more BC/sulfate when the AOD of BC/sulfate is
262 larger than the 75th percentile of itself in all rainy days, and cases with less BC/sulfate when that is less than
263 the 25th percentile of itself in the same situation. Accordingly, we selected 459 heavy rainfall cases with more
264 BC and 274 cases with less BC. Similarly, 361 cases with more sulfate and 419 cases with less sulfate were
265 selected (Fig. 6).

266 The SH at 850 hPa is used as the indicator of moisture [condition](#) under the cloud base. We chose wet cases
267 when the SH on that day is larger than 75th percentile of the whole rainy days, and chose dry cases when SH
268 on that day is less than the 25th percentile of the whole rainy days (the thresholds are shown in Tab. 1).

269 2.2.3 Statistical analysis

270 We adopted the probability distribution function (PDF) to compare the features of heavy rainfall and cloud
271 variables on different conditions of aerosols, through which we can understand the changes of rainfall/cloud
272 properties more comprehensively. The numbers of bins we selected in the study have been all tested for better
273 representing the PDF distribution. Student's t-test is used to examine the [statistical](#) significance level of [the](#)

Siyuan 20/2/19 11:34 PM

已删除: 630/716

Siyuan 20/2/19 11:34 PM

已删除: supply

276 differences or correlations between the different groups variables.

277

278 3. Changes of heavy rainfall

279 In this study, we applied two indicators (AOD and CDNC) to identify the aerosol pollution. AOD is usually
280 used as the macro indicator of aerosol pollution, which represents the optical feature of aerosol particles, rather
281 than the micro CCN (Shinozuka et al., 2015). To better identify the aerosol-cloud interaction, we intentionally
282 applied the CDNC as the indicator of CCN (Zeng et al., 2014; Zhu et al., 2018).

283 We first investigated the value distribution of AOD and CDNC over the BTH region. Figure 2a&b shows
284 the PDFs of AOD and CDNC on the non-rainfall days, rainfall days and heavy rainfall days respectively. We
285 found that the ranges of AOD values under the above three conditions are almost similar that is between 0-5
286 and their probability peaks all occur at around 1.2 (Fig. 2a). In contrast, CDNC shows different ranges among
287 the three conditions, which ranges from around 30 cm^{-3} to 600 cm^{-3} on the rainfall days and heavy rainfall
288 days, while from around 50 cm^{-3} to 800 cm^{-3} on the non-rainfall days. Besides, the proportion of low CDNC is
289 relatively high on the non-rainfall days (Fig. 2b). Accordingly, the range of AOD remains similar while the
290 range of CDNC is shortened on the rainfall days, probably because the cloud droplets become larger on
291 rainfall days, which could cause the reduction of number concentration. Therefore, to obtain comparable
292 samples, we use percentile method to select respective clean and polluted cases based on above two indicators
293 in order to better compare the characteristics of heavy rainfall. Hence the heavier pollution corresponds to
294 larger optical amount of aerosols measured by AOD, and more amount of aerosols that could serve as CCN
295 measured by CDNC.

296 3.1 Characteristics

297 Our previous study (Zhou et al. 2018) has reported the distinct peak shifts of rainfall diurnal variation between
298 clean and polluted days using the indicator of AOD over the BTH region during early summer. Similar with
299 our previous study, the PDF of the heavy rainfall peak time shows that the maximum of rainfall peak is about
300 two hours earlier on the polluted days (20:00 LST) than that on the clean days (22:00 LST) (Fig. 3a). To
301 comprehensively recognize the changes of rainfall diurnal variation associated with air qualities, here we
302 examined the PDF of the start time, the duration and the intensity besides the peak time of heavy rainfall.

303 As shown in Fig. 3a, the start time of heavy rainfall exhibits a significant advance on the polluted days. The
304 secondary peak on the early morning is ignored here because the early-morning rainfall is usually associated
305 with the mountain winds (Wolyn et al., 1994; Li et al., 2016) and the nighttime low-level jet (Higgins et al., 1997;
306 Liu et al., 2012) that is beyond the scope of this study. The time for the maximum frequency of heavy rainfall
307 initiation is around 6 hours earlier on the polluted days, shifting from around 0:00 LST on the clean days to
308 the 18:00 LST (Fig. 3a). Regarding the rainfall durations, the average persistence of heavy rainfall on polluted
309 days is 0.8 hours longer than that on clean days (Tab. 2). According to the PDF shown as in Fig. 3a, the

Siyuan 20/2/19 11:34 PM
已删除: of aerosol conditions. The differences between any two groups that have passed 95% statistical confidence level are considered significant. And two ... variables are cc...

Siyuan 20/2/19 11:34 PM
已设置格式: 字体:加粗

Siyuan 20/2/19 11:34 PM
已删除: used... pplied two indicators...

Siyuan 20/2/19 11:34 PM
已删除: The spectral distributions ...

Siyuan 20/2/19 11:34 PM
已设置格式: 字体颜色: 文字 1

Siyuan 20/2/19 11:34 PM
已删除:while from around 50 cm...

358 occurrence of short-term precipitation (≤ 6 hours, Yuan et al., 2010) decreases while that of long-term
359 precipitation (>6 hours, Yuan et al., 2010) increases. The intensity of hourly rainfall exhibits a non-significant
360 increase on the polluted days.

361 The distinct behaviors of heavy rainfall diurnal variation between clean and polluted days have been well
362 demonstrated using the indicator of AOD. Using CDNC as the indicator of CCN, the above-mentioned results
363 are also significant, as shown in Fig. 3b. The start time and peak time of heavy rainfall on the polluted
364 condition also show significant advances compared with that on the clean condition, with the average
365 advances of 2.2 hours and 2.6 hours respectively (Tab. 2). The duration of heavy rainfall on the polluted
366 condition is also prolonged, which is 0.5 hours longer in average (Tab. 2). Similar with the results based on
367 AOD, the difference of rainfall intensity between clean and polluted conditions using CDNC does not pass the
368 95% statistical confidence level as well.

369 Hence, the results using either AOD or CDNC show that the start and peak time of heavy rainfall occur
370 earlier and the duration becomes longer under pollution. We found the AOD and CDNC only have a
371 non-significant positive correlation, which denotes that the selected cases could be different between using
372 AOD and CDNC. The differences between the two indicators might be attributed to the non-linear
373 relationship between CCN and aerosol pollution (e.g., Jiang et al., 2016), the misdetection of AOD when the
374 humidity is high (Boucher and Quaas, 2012), the calculation uncertainty of CDNC, and the sampling
375 differences between AOD and CDNC. Since the two indicators represent aerosols from the different
376 perspectives, we cannot identify which one is more reliable. Because the change of rainfall intensity is not
377 significant based on either AOD or CDNC, the following analysis only focuses on studying the changes of
378 start time, peak time and duration of heavy rainfall along with aerosol pollution.

379 3.2 Sensitivities to aerosol types

380 Using the indicator of AI, we further investigated the distinct behaviors of heavy rainfall diurnal variation
381 related to absorbing aerosols and scattering aerosols respectively. The PDF of start time, peak time and
382 duration of heavy rainfall under the extreme circumstances of absorbing aerosols and scattering aerosols are
383 compared in Fig. 4. Here, we briefly named the days with extreme large amount of absorbing aerosols as
384 absorbing aerosol days and with more scattering aerosols as scattering aerosol days. The start time of heavy
385 rainfall on absorbing aerosol days shows a significant earlier compared with that on scattering aerosol days
386 (Fig. 4a), with 0.7 hours advance in average (Tab. 3). Similarly, the rainfall peak time also shows earlier on
387 absorbing aerosol days (Fig. 4b), with an average advance of 1.6 hours (Tab. 3). The rainfall duration on
388 scattering aerosol days shows longer than that on absorbing aerosol days, which are 6.0 hours and 5.0 hours
389 respectively in average (Tab. 3). All the above-mentioned differences between the two groups have passed 95%
390 statistical confidence level. The results indicate that the absorbing aerosols and scattering aerosols may have
391 different or inverse effects on the heavy rainfall that absorbing aerosols may generate the heavy rainfall in
392 advance while the scattering aerosols may delay and prolong the heavy rainfall.

Siyuan 20/2/19 11:34 PM

已删除: 1.4

Siyuan 20/2/19 11:34 PM

已删除: 3.0

Siyuan 20/2/19 11:34 PM

已删除: 2.2

Siyuan 20/2/19 11:34 PM

已删除: , although there are some quantitative differences between the two indicators.

Siyuan 20/2/19 11:34 PM

已删除: The cases of heavy rainfall using CDNC seem more extreme, because the rainfall behaviors exhibit more evident changes using CDNC than using AOD. The result

Siyuan 20/2/19 11:34 PM

已删除: using

404 To further verify the different behaviors of heavy rainfall diurnal variation associated with two different
405 types of aerosols, we purposely re-examine the above-mentioned phenomena using BC/sulfate that can
406 represent typical absorbing/scattering aerosols over the BTH region. BC has its maximum center over BTH
407 region (Fig. 5a) and our previous study has indicated that the radiative effect of BC low-level warming may
408 facilitate the convective rainfall generation (Zhou et al., 2018). The percentage of sulfate is also large over the
409 BTH region (Fig. 5b) and sulfate is one of the most effective CCN that influences the precipitation in this
410 region (Gunthe et al., 2011). Accordingly, we selected the cases with different amounts of BC and sulfate
411 AOD to compare their roles on the diurnal variation of heavy rainfall. The methods have been described in
412 Sect. 2.2.2. The PDF of the start time, peak time and duration of heavy rainfall in the cases with more/less
413 amount of BC are shown in Fig. 6a, respectively. The most striking result is that the maximum frequency of
414 rainfall start time in the more BC cases evidently shifts earlier (Fig. 6a). Meanwhile, the mean peak time in
415 the more BC cases shows 1.1 hour earlier than that in the less BC cases (Tab. 3). And the duration of heavy
416 rainfall is slightly shortened by the averaged 0.2 hours in the more BC cases. The features in more BC cases
417 are consistent with the above results of absorbing aerosols. In contrast, when the sulfate has larger amount, the
418 mean start time of rainfall is delayed by 0.5 hours, while the duration shows a significant increase by 1.5
419 hours in average (Tab. 3). The behaviors in the more sulfate cases also exhibit similar with the above results
420 of scattering aerosols, except for the peak time that shows later in the scattering aerosol cases but a little
421 earlier in the more sulfate cases (Tab. 3).

422 3.3 Influence of moisture

423 Moisture supply is an indispensable factor for the precipitation formation, and it also has an important impact
424 on AOD (Boucher and Quaas, 2012). Since the southwesterly circulation can not only transport pollutants but
425 also plenty of moisture to the BTH region (Wu et al., 2017), more pollution usually corresponds to more
426 moisture for the BTH region (Sun et al., 2015) so that it is hard to completely remove the moisture effect on
427 the above results in a pure observational study. Here we attempt to recognize the moisture effect on the heavy
428 rainfall to further understand the above aerosol-associated changes. Because the moisture supply for BTH is
429 mainly transported via low-level southwesterly circulation, we purposely used the SH at 850 hPa as the
430 indicator of moisture condition.

431 Using the similar percentile method with polluted/clean days, we compared the heavy rainfall
432 characteristics in the more humid (more than 75th percentile) and the less humid (less than 25th percentile)
433 environments regardless of the aerosol condition, as shown in Fig. 7a. The results show that the start time of
434 heavy rainfall is delayed by 0.9 hours, the peak time is 0.6 hours earlier and the duration is prolonged by 2.0
435 hours in average in the more humid environment, which is similar with the results of the more sulfate cases.
436 Besides, the same results are obtained using different moisture indicator, e.g. the 850 hPa absolute humidity.
437 These results indicate the advance of heavy rainfall start time on the polluted days is not caused by more
438 moisture supply, while the longer duration and earlier peak in the more sulfate cases might be related to the

Siyuan 20/2/19 11:34 PM

已删除: the

Siyuan 20/2/19 11:34 PM

已删除: higher

Siyuan 20/2/19 11:34 PM

已删除: the

442 increased moisture supply. To further identify the role of sulfate, we examined the sensitivities of the results
443 associated with sulfate under different moisture condition. In the dry (SH less than 25th percentile) and
444 intermediate cases (SH between 25th - 75th percentiles), the heavy rainfall still shows later start time, earlier
445 peak and significant longer duration with the increase of sulfate, while the change of peak time is not
446 significant in the dry cases; in the high moisture cases (SH more than 75th percentile), it shows earlier peak
447 and shorter duration in the more sulfate cases while the change of start time is not significant. Therefore, we
448 suppose that the impact of sulfate aerosols on the heavy rainfall is sensitive to moisture, and notably the
449 sulfate could contribute to the longer duration in the polluted cases when it is relatively dry.

Siyuan 20/2/19 11:34 PM
已删除: tested...xamined the sensitivi... [5]

450 We also investigate the distributions of moisture and rainfall behaviors in the clean and polluted cases
451 respectively using AOD and CDNC (Fig. 7 b&c). The results show that the relationship between moisture and
452 rainfall start time/peak time/duration is not linear. The distribution of SH exhibits a slight increase with
453 pollution in the AOD cases, indicating that the polluted cases selected by AOD are accompanied with more
454 moisture than the clean cases. However, when fixing the moisture at a certain range especially at the relative
455 dry condition, (for example, the SH between 8-12 g/kg), we can detect the similar phenomena of earlier
456 start/peak time and longer duration in the polluted cases based on either AOD or CDNC. To further clarify the
457 characteristics of heavy rainfall associated with pollution, we removed the samples with high SH (SH more
458 than 75th percentile) and found that the results in section 3.1 remain, that is the start/peak time of heavy
459 rainfall is in advance and the duration is prolonged with the increase of AOD/CDNC when SH is less than
460 12.95 g/kg (75th percentile) (Fig. 8).

Siyuan 20/2/19 11:34 PM
已删除: Using either AOD or CDNC... [6]

461 The above results indicate that the advance of heavy rainfall start in the polluted cases is independent of
462 moisture condition, while the advance of peak time and longer duration could be influenced by the moisture
463 effect. For the earlier peak time of heavy rainfall, we suppose the role of BC (absorbing aerosols) might be
464 dominant because the change of peak time in the former analysis is more significant (Tab. 3) although the
465 sulfate and moisture also have positive contribution. The increased sulfate (scattering aerosols) contributes to
466 the longer duration of heavy rainfall (Fig. 6b), but the role of sulfate is kind of sensitive to the moisture
467 condition. With the increase of sulfate, the duration is longer when the moisture condition is relatively dry
468 while becomes shorter when it is extremely wet. Overall, when removing the extremely high moisture cases,
469 the earlier start/peak time and longer duration of heavy rainfall associated with aerosol pollution are
470 significant.

Siyuan 20/2/19 11:34 PM
已删除: might...ould be related [7]

472 4. Changes of clouds

473 To understand the cloud effect of aerosols during heavy rainfall diurnal variation, we need to recognize the
474 associated cloud characteristics on the clean and polluted conditions. The cloud properties we used were
475 obtained from satellite product that was measured at the same time with aerosols before the occurrence of

Siyuan 20/2/19 11:34 PM
已删除: were [8]

521 heavy rainfall. The differences of cloud features were examined in both macroscopic (including CF, CTP,
522 COT and CWP) and microscopic properties (including CER) on the clean and polluted conditions based on
523 AOD and CDNC respectively.

Siyuan 20/2/19 11:34 PM

已删除: between

524 4.1 Characteristics

525 Using AOD as the macro aerosol indicator, as shown in Fig. 9, the PDF distribution shows that the CF on the
526 polluted condition is evidently larger than that on the clean condition. The average CF is 62.8% on the clean
527 condition, and 89.3% on the polluted condition (Tab. 4). The average CTP on the polluted condition is 487.3
528 hPa, which is larger than 442.3 hPa on the clean condition, indicating that the cloud top height is lower on the
529 polluted days. The COT, CWP and CER were further analyzed for the liquid and ice portions of clouds as
530 shown in Fig. 9. Both liquid and ice COT on the polluted condition exhibit significant increases compared
531 with that on the clean condition. The mean amount of liquid COT is increased by 3.1 and ice COT increases
532 by 6.2 (Tab. 4). Similar with COT, the amounts of liquid and ice CWP also increase under pollution, which
533 increase by 33.6 g/m² and 88.2 g/m² respectively. In addition, the liquid CER is increased by 0.8 μm and the
534 ice CER is decreased by 2.8 μm on the polluted days. The differences of above cloud properties between clean
535 and polluted cases have all passed the 95% statistical confidence level.

Siyuan 20/2/19 11:34 PM

已删除: of CF

Siyuan 20/2/19 11:34 PM

已删除: 4), which is increased by 26.1%.

536 Using CDNC as the micro aerosol indicator, the above-mentioned changes of cloud properties are
537 consistent with that using AOD, except for liquid CER (Fig. 9). Since the calculation method of CDNC is not
538 independent on the liquid COT and liquid CER, we would not directly compare the results of liquid COT and
539 CER based on CDNC with those based on AOD here. But according to other variables that are independent of
540 the CDNC calculation, we found the cases with more CDNC are accompanied with the increase of CTP, ice
541 COT and liquid & ice CWP, which increase by 90.2 hPa, 24.4, 112.4 g/m² and 224.1 g/m² respectively (Tab. 4)
542 and all of which are consistent with the results based on AOD. The CER of ice clouds also shows a consistent
543 decrease by 9.5 μm on the polluted condition based on CDNC. We noticed that the changes of
544 COT/CWP/CER for both liquid and ice based on CDNC are much larger than that based on AOD, which
545 indicates that these cloud properties might be more sensitive to the indicator of CDNC rather than AOD.

Siyuan 20/2/19 11:34 PM

已删除: 32.8

Siyuan 20/2/19 11:34 PM

已删除: 215.8

Siyuan 20/2/19 11:34 PM

已删除: 370.9

Siyuan 20/2/19 11:34 PM

已删除: 8.8

546 According to the above comparison, the concurrent changes of cloud properties along with heavy rainfall
547 diurnal variation show consistent results using the two aerosol indicators (AOD and CDNC). The pollution
548 corresponds to the increase of CF, ice COT, liquid and ice CWP, but the decrease of cloud top height (the
549 increase of CTP corresponds to the decrease of cloud top height) and ice CER. The liquid COT and liquid
550 CER are also increased with the enhanced pollution in the AOD analysis. Besides, the above-mentioned
551 results exhibit significant when we limited the moisture to the dryer condition (SH less than 25th percentile) or
552 intermediate condition (SH between 25th – 75th percentile). When the moisture is higher (SH more than 75th
553 percentile), the change of CTP become not significant based on CDNC.

Siyuan 20/2/19 11:34 PM

已删除: these

Siyuan 20/2/19 11:34 PM

已删除: more than

Siyuan 20/2/19 11:34 PM

已删除: percentile and less than

Siyuan 20/2/19 11:34 PM

已删除: does

Siyuan 20/2/19 11:34 PM

已删除: show

554 According to these results, we made the following speculation: First, the CF, liquid & ice COT and CWP

Siyuan 20/2/19 11:34 PM

已删除: For

568 increase with pollution, because the aerosols serving as CCN can nucleate a larger number of cloud droplets
 569 which in a moisture sufficient environment can hold more liquid water in the cloud. Second, the CTP
 570 increases (the cloud top height decreases) under pollution using both AOD and CDNC, because the earlier
 571 start of the precipitation process (Fig. 3) inhibits the vertical growth of clouds. Third, the ice CER decreases
 572 under pollution using either AOD or CDNC, because the increased cloud droplet number leads to more cloud
 573 droplets transforming into ice crystals and causes the decrease of ice CER (Chylek et al., 2006; Zhao et al.,
 574 2018; Gryspeerdt et al., 2018). However, the results of liquid CER might have uncertainties. The liquid CER
 575 is increased when AOD increases (Fig. 9), which might be related to the aerosol humidification effect, the
 576 misdetection of AOD and cloud water, and the earlier formation of the clouds and precipitation on the polluted
 577 days. Since we cannot distinguish the liquid part of mix-phased clouds from liquid (warm) clouds in the
 578 observation, the above-mentioned change of liquid cloud properties might come from that of both the liquid
 579 (warm) clouds and the liquid part of mixed-phase clouds. Likewise, the above-mentioned change of ice cloud
 580 properties might come from that of both ice (cold) clouds and the ice part of mixed-phase clouds. Currently
 581 the physical processes of cold clouds and mixed-phase clouds have been not clarified yet, including the
 582 diffusional growth, accretion, riming and melting process of ice precipitation (Cheng et al., 2010), which
 583 needs numerical model simulations to be further explored.

584 4.2 Sensitivities to CCN (represented by CDNC) and moisture

585 Section 3.3 has shown that the diurnal variation of heavy rainfall with more moisture supply is similar with
 586 the changes of heavy rainfall with more sulfate aerosols. We assume that the moisture under the cloud base
 587 and the sulfate serving as CCN both influence the cloud properties (Yuan et al., 2008; Jiang et al., 2008; Jung
 588 et al., 2013; Qiu et al., 2017). To identify the effect of CCN on clouds and its sensitivity to moisture, using
 589 CDNC to represent CCN, we purposely investigated the changes of above cloud properties on the different
 590 conditions of the CDNC and the low-level moisture (850hPa SH) respectively.

591 We categorized all cases of heavy rainfall into four groups, which are (1) clean and dry, (2) polluted and
 592 dry, (3) clean and wet, (4) polluted and wet, and checked the changes of above cloud properties, as shown in
 593 Tab. 5. To retrieve the comparable samples, here “clean/polluted” refers to the CDNC on that day less/more
 594 than 25th/75th percentile of the CDNC among the heavy rainfall days, and similarly, the “dry/wet” refers to the
 595 SH on that day less/more than 25th/75th percentile of itself among the heavy rainfall days. The average CDNC
 596 is 125.54 cm⁻³ on the dry condition and 120.71 cm⁻³ on the wet condition, and the average SH is 11.62 g/kg
 597 and 11.73 g/kg on the clean and polluted conditions respectively, thus we consider the CDNC or SH remain
 598 almost the same when the other condition changes. We tested the significance of differences between group 1
 599 and 2, group 1 and 3, group 2 and 4, group 3 and 4. Because the CF is fixed above 80% when calculating the
 600 CDNC (see in Sect. 2.1.3), here the selected groups all belong to the condition of higher CF.

601 Comparing the results of group 1 and 2, which are both on the dry condition, we can identify the influence
 602 of CDNC on the cloud properties, which represents the effect of CCN. The changes of these cloud variables

- Siyuan 20/2/19 11:34 PM
已删除: might
- Siyuan 20/2/19 11:34 PM
已删除: and accumulate
- Siyuan 20/2/19 11:34 PM
已删除: thus increase the CF, COT and CWP.
- Siyuan 20/2/19 11:34 PM
已删除: which denotes the decrease of the cloud top height, might
- Siyuan 20/2/19 11:34 PM
已删除: probably
- Siyuan 20/2/19 11:34 PM
已删除: also might result from
- Siyuan 20/2/19 11:34 PM
已删除: heavy rainfall
- Siyuan 20/2/19 11:34 PM
已删除: changes
- Siyuan 20/2/19 11:34 PM
已删除: changes
- Siyuan 20/2/19 11:34 PM
已删除: detailed
- Siyuan 20/2/19 11:34 PM
已删除: grow

- Siyuan 20/2/19 11:34 PM
已删除: 68.58
- Siyuan 20/2/19 11:34 PM
已删除: 68.56
- Siyuan 20/2/19 11:34 PM
已删除: 3
- Siyuan 20/2/19 11:34 PM
已删除: 8
- Siyuan 20/2/19 11:34 PM
已删除: can
- Siyuan 20/2/19 11:34 PM
已删除: remains
- Siyuan 20/2/19 11:34 PM
已删除: made
- Siyuan 20/2/19 11:34 PM
已删除: significant test
- Siyuan 20/2/19 11:34 PM
已删除: stands for

625 are the same as that in Sect. 4.1, that the CF, ice COT and liquid & ice CWP are increased on the polluted
626 condition, while the cloud top height and ice CER are decreased based on CDNC. Among these variables, the
627 ice COT and liquid & ice CWP are especially larger on the polluted condition, which are 3-4 times larger than
628 that on the clean condition (Tab. 5). On the wet condition, comparing the group 3 and 4, the changes are
629 similar that the CF, ice COT and liquid & ice CWP are increased and the ice CER are decreased but the
630 change of CTP becomes not significant. However, the changes of these variables on the dry condition are
631 evidently enhanced than that on the wet condition, which indicates these cloud properties might be more
632 sensitive to CDNC on the dry condition. The above comparisons indicate that with the increase of CDNC
633 (CCN), the CF, ice COT and liquid & ice CWP are increased while the ice CER is decreased regardless of the
634 moisture amount.

Siyuan 20/2/19 11:34 PM

已删除: 5-6

635 Comparing the results of group 1 and 3, we can get the changes of cloud properties related only to moisture
636 on the same clean condition. A common feature is that CF, CTP, COT and CWP both for liquid and ice exhibit
637 increases along with the increase of moisture. Compared with the CTP on the clean and dry condition, it
638 increases on both polluted & dry condition (group 2) and clean & wet condition (group 3), but on the former
639 condition its increase is larger, which indicates the influence of moisture on CTP might be secondary
640 compared to the CDNC (CCN) effect. Similarly, comparing the COT/CWP in group 2 and 3, the increases of
641 COT and CWP both for liquid and ice in group 2 are much larger than that in group 3, which indicates that the
642 influences of moisture on COT and CWP may not overcome the influence of CCN. With the increase of
643 moisture, the change of liquid CER is not significant on the same clean condition, but the ice CER is
644 significantly decreased. On the polluted condition, comparing group 2 and 4, we found the COT and CWP
645 both for liquid and ice on the wet condition are evidently smaller than that on the dry condition, which
646 indicates that increasing the moisture might partly compensate for the influence of CDNC (CCN) on
647 COT/CWP. Besides, the liquid CER exhibits a slight increase with increased moisture in the same polluted
648 environment, which may further support the idea that the increased CCN could nucleate more cloud water
649 with increased moisture.

Siyuan 20/2/19 11:34 PM

已删除: Although the comparisons of liquid COT and liquid CER based on CDNC are meaningless since the CDNC is calculated by the two variables, we infer that the increase of liquid COT and the decrease of liquid CER (Tab. 5) might be not completely caused by CDNC calculation but the natural effect of CCN.

650 The results above indicate that both CDNC (CCN) and moisture have impacts on cloud properties. They
651 both contribute to the increase of CF, CTP, COT and CWP, in which the influence of CDNC (CCN) on COT
652 and CWP are significantly larger than moisture. Both CDNC and moisture correspond to the significant
653 decrease of ice CER, while only CDNC corresponds to the decrease of liquid CER and that might be ascribed
654 to the calculation method of CDNC. To reduce uncertainties, we have tested the SH at different levels (e.g.,
655 700 hPa and 800 hPa) and different moisture indicator (e.g. absolute humidity) to verify these results, and
656 found most cloud variables show the similar changes with above except for the CTP and the liquid CER,
657 which indicates the changes of CTP and liquid CER are more sensitive and have larger uncertainties. Since
658 the behaviors of cloud changes are similar along with the increase of either CDNC (CCN) or moisture but
659 more sensitive to the former, the results in Sect. 4.1 might actually reflect the combined effect of CCN and
660 moisture, and the aerosol (CCN) effect on these cloud properties might be dominant on the polluted days.

Siyuan 20/2/19 11:34 PM

已删除: 3-6 times

Siyuan 20/2/19 11:34 PM

已删除: The increase of either CDNC or moisture corresponds to the increase of CTP. But when the CDNC and moisture increase simultaneously, the CTP becomes smaller.

675 Therefore, considering the results from this subsection and Sect. 3.3 that the changes of cloud features
676 become smaller in the higher moisture environment than that in the dryer environment and the duration of
677 heavy rainfall is relatively shortened with pollution when it is extremely wet (Sect. 3.3), we speculate that the
678 sulfate (CCN) effect might be suppressed in a relatively wet environment. Due to the limitations of
679 observational study, we currently cannot figure out the respective roles of aerosols and moisture.

680

681 5. Hypothesis

682 According to all the above results, we have made hypotheses about the aerosol effects on the heavy rainfall
683 over the BTH region. In Sect. 3.1 we found that the heavy rainfall has earlier start and peak time, and longer
684 duration on the polluted condition. And afterwards, the earlier start of rainfall under pollution was found
685 related to absorbing aerosols mainly referring to BC (Fig. 4a&6a). We also compared the effect of BC on the
686 associated clouds. Figure 10a shows the CF larger than 90% rarely occurs in the more BC environment, which
687 might be associated with the semi-direct effect of BC (Ackerman, 2000) or estimated inversion strength and
688 BC co-vary. This result indicates the influence of BC on the heavy rainfall in Fig. 6a is mainly due to the
689 radiative effect rather than the cloud effect. The mechanism of BC effect on the heavy rainfall can be
690 interpreted by our previous study (Zhou et al., 2018) as: BC absorbs shortwave radiation during the daytime
691 and warms the lower troposphere at around 850 hPa, and then increases the instability of the lower to middle
692 atmosphere (850-500 hPa) so that enhances the local upward motion and moisture convergence. As a result,
693 the BC-induced thermodynamic instability of the atmosphere triggers the occurrence of heavy rainfall in
694 advance. Thus, the low-level heating effect of BC might play a dominant role in the beginning of rainfall
695 especially before the formation of clouds during the daytime.

696 The delayed start of heavy rainfall with scattering aerosols in Fig. 4a and more sulfate in Fig. 6b is
697 consistent with many studies that both the radiative effect and cloud effect of sulfate-like aerosols could delay
698 or suppress the occurrence of rainfall (Guo et al., 2013; Wang et al., 2016; Rosenfeld et al. 2014). Sulfate-like
699 aerosols as scattering aerosols could prevent the shortwave radiation from arriving at the surface thus cool the
700 surface and stabilize the atmosphere, which suppresses the rainfall formation (Guo et al., 2013; Wang et al.,
701 2016). Sulfate-like aerosols serving as CCN can also suppress the rainfall by cloud effect through reducing the
702 cloud droplet size and thus suppressing the collision-coalescence process of cloud droplets (Albrecht 1989;
703 Rosenfeld et al. 2014). Figure 10b does shows that in contrast with BC, the CF larger than 90% is
704 significantly increased in the more sulfate environment, which indicates the sulfate-like aerosols might have
705 more evident influence on the clouds and subsequently the rainfall changes associated with sulfate are
706 probably due to the cloud effects. Another significant feature is the longer duration of heavy rainfall in the
707 scattering aerosol cases, more sulfate cases and high moisture cases (Fig 4c, 6b&7a). We speculate that the
708 longer duration is caused by both the cloud effect of sulfate-like aerosols and the increased moisture supply,
709 because increasing either CCN or the moisture supply can increase cloud water (Sect. 4.2), which could lead

Siyuan 20/2/19 11:34 PM

已删除: Therefore, combining with the results in Sect. 3.3, although we cannot completely separate the aerosols and moisture, the CCN is assumed to play a vital role on the clouds and precipitation especially in a relatively dry environment. In the relatively wet environment, the CCN might have some inhibitory effect since the duration of heavy rainfall is shorter with the increase of sulfate when it is extremely wet, and the changes of cloud features along with the CDNC increase are smaller on the wet condition.

Siyuan 20/2/19 11:34 PM

已删除: 500hPa

Siyuan 20/2/19 11:34 PM

已删除: the postponed start of heavy rainfall is mainly due to the effect of sulfate-like aerosols, while

726 to the longer rainfall duration. To further investigate the mechanism of longer duration, we need the assistance
727 of numerical model simulations in the future work.

728 Accordingly, we speculate that the earlier start time of heavy rainfall related to absorbing aerosols (BC) is
729 due to the radiative heating of absorbing aerosols, while the longer rainfall duration is probably caused by
730 both the cloud effect of sulfate-like aerosols and the increased moisture supply. As a summary we use a
731 schematic diagram (Fig. 11) to illustrate how aerosols modify the heavy rainfall in the meteorological
732 background of southwesterly over the BTH region. On one hand, BC heats the lower troposphere, changing
733 the thermodynamic condition of atmosphere, which increases the upward motion and accelerates the
734 formation of clouds and rainfall. On the other hand, the increased upward motion transports more sulfate-like
735 particles and moisture into the clouds so that the increased aerosols serving as CCN could nucleate more cloud
736 water, thus prolong the duration of rainfall. As a result, the earlier start and peak time, and longer duration of
737 heavy rainfall over BTH region might due to the combined effect of aerosol radiative effect, aerosol cloud
738 effect. To further verify the individual effect, we need to conduct numerical model simulations in our future
739 study.

740

741 6. Discussion and conclusions

742 6.1 Discussion

743 In this study we used two aerosol indicators, AOD and CDNC, which discriminates the pollution levels for
744 different purposes. AOD is a good proxy for the large-scale pollution level, but it stands for the optical feature
745 of aerosols and cannot well represent CCN when we focused on the aerosol-cloud interaction (Shinozuka et al.,
746 2015). CDNC is a better proxy for CCN compared with AOD, which facilitates the study on the cloud changes
747 associated with aerosol pollution. But the retrieved CDNC has larger uncertainties. First, the assumptions in
748 the calculation of CDNC are idealized that CDNC is constant with height in a cloud and cloud liquid water
749 increases monotonically at an adiabatic environment (Grosvenor et al., 2018), but the target of this study is the
750 convective clouds with rainfall that may be not consistent with the adiabatic assumption. Second, as indicated
751 by Grosvenor et al. (2018), the uncertainties in the pixel-level retrievals of CDNC from MODIS with 1°x1°
752 spatial resolution can be above 54%, which come from the uncertainties of parameters and the original COT
753 and CER data using in the calculation, and also the influence of heterogeneity effect from thin clouds. To
754 reduce the influence of heterogeneity effect as much as possible, we have attempted to limit the conditions of
755 CF, liquid COT and CER when calculating CDNC in the study. Besides, this study primarily focuses on the
756 relative changes of CDNC, which may be also influenced by the potential systematic biases in the CDNC
757 calculation, but actually reduced the uncertainties of absolute values. Another problem about CDNC in this
758 study is that the CDNC could be influenced by updraft velocity because both increased CCN and updraft
759 velocity could enhance aerosol activation and increase CDNC (Reutter et al., 2009). Since we cannot get any

Siyuan 20/2/19 11:34 PM
已删除: CCN and sufficient moisture increase the

Siyuan 20/2/19 11:34 PM
已删除: might

Siyuan 20/2/19 11:34 PM
已删除: heavy rainfall over BTH region in southwesterly shows

Siyuan 20/2/19 11:34 PM
已删除: as well as the moisture effect.

Siyuan 20/2/19 11:34 PM
已删除: distinguish

Siyuan 20/2/19 11:34 PM
已删除: Conclusions

Siyuan 20/2/19 11:34 PM
已删除: discussion

Siyuan 20/2/19 11:34 PM
已删除: Based on macro and micro aerosol indicators that are AOD from MODIS aerosol product and calculated CDNC from MODIS cloud product, we found three features of heavy rainfall changing associated with aerosols that the rainfall start and peak time occur earlier and the duration becomes longer. The quantitative differences exist between the two indicators, i.e., the statistic differences of above features between clean and polluted conditions are 0.7, 1.0, 0.8 hours based on AOD and 1.4, 3.0, 2.2 hours based on CDNC.

Siyuan 20/2/19 11:34 PM
已删除: of

Siyuan 20/2/19 11:34 PM
已删除: is actually

Siyuan 20/2/19 11:34 PM
已删除: when we use CDNC to represent CCN since

Siyuan 20/2/19 11:34 PM
已删除: contribute to

Siyuan 20/2/19 11:34 PM
已删除: We

788 in-cloud long-term updraft data, we used the vertical velocity at 850 hPa obtained from ERA-interim
789 reanalysis data to roughly represent the cloud base updraft and investigated the possible relationship between
790 CDNC and updraft. The results show that there is no significant correlation between CDNC and vertical
791 velocity, although the updraft is relatively intensified in the polluted cases. We also examined the change of
792 rainfall based on CDNC under three certain ranges of vertical velocity (less than 25th percentile, between 25th
793 75th percentile and more than 75th percentile), and found the primary results are similar.

Siyuan 20/2/19 11:34 PM
已删除: investigate ...oughly repre... [9]

Siyuan 20/2/19 11:34 PM
已设置格式: 字体颜色: 红色

794 In addition to AOD and CDNC, we also applied ultraviolet AI and AOD of BC/sulfate to identify different
795 types of aerosols. We found that the AI has a weak positive correlation with AOD from MODIS, which
796 indicates the results on absorbing aerosol days might represent the results on polluted days if identified by
797 AOD. To avoid the uncertainty, we re-examined the results using AI when removing the polluted cases
798 identified by AOD, and found the major results remain. The comparisons of BC/sulfate AOD cases also have
799 uncertainties because they are retrieved from MACC reanalysis data. Although the above four indicators have
800 their own uncertainties, currently we cannot find more reliable datasets in a long-term observational record.
801 The major findings using these four indices could well identify the changes of rainfall and clouds
802 accompanied with aerosols, but are insufficient to clarify the aerosol effect on clouds and precipitation.

Siyuan 20/2/19 11:34 PM
已删除: are not changed.

803 This study has clearly identified the relationship of the aerosol pollution and the diurnal changes of heavy
804 rainfall and associated clouds in the BTH region. However, although this work has attempted to exclude the
805 impacts from the meteorological background particularly circulation and moisture, the observation study still
806 has its limitations on studying aerosol effects on rainfall and clouds: first, the observational datasets have their
807 noise and uncertainty, including the misdetection of CF in the satellite product when AOD is large (Brennan et
808 al., 2005; Levy et al., 2013) and the mutual interference between liquid and ice clouds (Holz et al., 2008;
809 Platnick et al., 2017); Second, the meteorological co-variations cannot be completely removed thus bring the
810 uncertainties of the results, e.g., the meteorology might affect the relationship between AOD and CF (Quaas et
811 al., 2010; Grandey et al., 2013) and the relationship between AOD and CTP (Gryspeerd et al., 2014a); Third,
812 the different types of aerosols cannot be completely well separated, although we used AI index and AOD of
813 BC/sulfate to identify the respective effects of absorbing aerosols and scattering aerosols. In addition, we
814 selected the extreme ranges of AOD/CDNC to compare the characteristics of heavy rainfall and associated
815 clouds, which could bring such uncertainties that these extreme conditions might be related with distinct
816 microphysical process or meteorological background. We further examined the results using the middle range
817 of AOD and CDNC such as 25th – 50th percentile versus 50th -75th percentile. The results are basically the same
818 except that the peak time change is not significant based on AOD. Numerical model simulations are
819 necessarily applied to further study the specific impact of aerosols on the heavy rainfall. And the detailed
820 processes of aerosol effect on the precipitation formation of mix-phased and cold clouds also needs further
821 exploration in our future study.

Siyuan 20/2/19 11:34 PM
已删除: of different observational data
cannot be avoid, e.g.,... including th... [10]

822 **6.2 Conclusions**

871 Using the gauge-based hourly rainfall records, aerosol and cloud satellite products and high temporal
872 resolution reanalysis datasets during 2002-2012, this study investigated the different characteristics of heavy
873 rainfall in the diurnal time scale on the clean and polluted conditions respectively. Based on the macro and
874 micro aerosol indicators including AOD from MODIS aerosol product and calculated CDNC from MODIS
875 cloud product, three significant features of heavy rainfall diurnal change associated with aerosols are found,
876 that is the rainfall start and peak time occur earlier and the duration becomes longer under pollution.

877 The different relationships of absorbing and scattering aerosols with the heavy rainfall diurnal shift were
878 distinguishable using ultraviolet AI from OMI and reanalysis AOD of two aerosol types (BC and sulfate). The
879 absorbing aerosols (BC) correspond to the earlier start and peak time of heavy rainfall, while the scattering
880 aerosols (sulfate) correspond to the delayed start time and the longer duration. [Considering the plausible effect
881 of moisture, further](#) analysis indicates the duration of heavy rainfall is prolonged in the presence of more
882 sulfate on the relatively dry condition but is shortened on the extremely wet condition.

883 By comparing the characteristics of cloud macrophysics and microphysics variables, using both AOD and
884 CDNC we found the CF, ice COT, liquid and ice CWP are increased on the polluted condition, but the cloud
885 top height and the ice CER are reduced. Liquid COT and liquid CER are also increased in AOD analysis.
886 Comparing the influences of CDNC which represents CCN and SH at 850 hPa which represents moisture
887 condition respectively on these cloud variables, the cloud properties show similar changes with the increase of
888 CDNC and moisture, but seem more sensitive to the CDNC (CCN), e.g., the liquid & ice COT and CWP [are
889 increased more significantly in high CDNC than in high SH.](#)

890 According to these results, we speculate that both aerosol radiative effect and cloud effect have impacts on
891 the diurnal variation of heavy rainfall in the BTH region. The heating effect of absorbing aerosols especially
892 BC increases the instability of the lower to middle atmosphere so that generates the heavy rainfall occurrence
893 in advance. [And the increased moisture supply and increased aerosols which could nucleate more cloud water
894 in the cloud, leading to the longer duration of heavy rainfall.](#)

895

896 **Data availability**

897 We are grateful to the National Meteorological Information Centre (NMIC) of the China Meteorological
898 Administration (CMA) for providing hourly precipitation datasets. MODIS aerosol and cloud data were
899 obtained from <http://ladsweb.modaps.eosdis.nasa.gov>; ultraviolet AI data from OMI was obtained from
900 <https://daac.gsfc.nasa.gov/datasets?keywords=OMI&page=1>; MACC-II and ERA-interim reanalysis datasets
901 were obtained from <http://apps.ecmwf.int/datasets>.

902 **Author contributions**

903 JY and SZ conceived the study. SZ processed data and drew the figures. SZ and JY analyzed the observational

904 results and WCW, CZ and DG gave the professional guidance. PS provided the hourly precipitation dataset.
905 SZ and JY prepared the manuscript with contributions from WCW and CZ.

906 **Competing interests**

907 The authors declare that they have no conflict of interest.

908 **Acknowledgements**

909 Jing Yang, Daoyi Gong & Peijun Shi are supported by funds from the National Natural Science Foundation of
910 China ([41775071](#) and [41621061](#)) and the National Key Research and Development Program-Global Change
911 and Mitigation Project: Global Change Risk of Population and Economic System: Mechanism and
912 Assessment (2016YFA0602401 and [2018YFC1505903](#)), Siyuan Zhou is supported by funds from State Key
913 Laboratory of Earth Surface Processes and Resource Ecology and Key Laboratory of Environmental Change
914 and Natural Disaster. Wei-Chyung Wang acknowledges the support of grants (to SUNYA) from the Office of
915 Sciences (BER), U.S. DOE and the U.S. National Science Foundation (1545917) in support of the Partnership
916 for International Research and Education project at the University at Albany. We deeply appreciate two
917 anonymous referees for their in-depth comments and constructive suggestions.

918

919 **References:**

- 920 Ackerman, A. S.: Reduction of Tropical Cloudiness by Soot, *Science*, 288, 1042-1047,
921 doi:10.1126/science.288.5468.1042, 2000.
- 922 Albrecht, B. A.: Aerosols, cloud microphysics, and fractional cloudiness, *Science*, 245, 1227-1230,
923 doi:10.1126/science.245.4923.1227, 1989.
- 924 Altaratz, O., Bar-Or, R. Z., Wollner, U., and Koren, I.: Relative humidity and its effect on aerosol optical
925 depth in the vicinity of convective clouds, *Environ. Res. Lett.*, 8, 034025,
926 doi:10.1088/1748-9326/8/3/034025, 2013.
- 927 Anonymous: Atmospheric Sciences Thesaurus, China Meteorological Press: Beijing, China, 1994. (in
928 Chinese)
- 929 Anonymous: IPCC fifth assessment report, *Weather*, 68, 310-310, 2013.
- 930 Bellouin, N., Quaas, J., Morcrette J. -J., and Boucher, O.: Estimates of aerosol radiative forcing from the
931 MACC re-analysis, *Atmos. Chem. Phys.*, 13, 2045-2062, doi:10.5194/acp-13-2045-2013, 2013.
- 932 Benedetti, A., Morcrette, J. J., Boucher, O., Dethof, A., Engelen, R. J., Fisher, M., Flentje, H., Huneeus, N.,
933 Jones, L., Kaiser, J. W., Kinne, S., Mangold, A., Razinger, M., Simmons, A. J., and Suttie, M.: Aerosol
934 analysis and forecast in the European Centre for Medium-Range Weather Forecasts Integrated Forecast
935 System: 2. Data assimilation, *J. Geophys. Res.*, 114, D13205, doi:10.1029/2008JD011115, 2009.
- 936 Brennan, J., Kaufman, Y., Koren, I., and Rong, L.: Aerosol-cloud interaction-Misclassification of MODIS
937 clouds in heavy aerosol, *IEEE T. Geosci. Remote*, 43, 911-915, doi:10.1109/TGRS.2005.844662, 2005.

939 Bennartz, R., and Rausch, J.: Global and regional estimates of warm cloud droplet number concentration
940 based on 13 years of AQUA-MODIS observations, *Atmos. Chem. Phys.*, 17, 9815-9836,
941 doi:10.5194/acp-17-9815-2017, 2017.

942 Bennartz, R.: Global assessment of marine boundary layer cloud droplet number concentration from satellite, *J.*
943 *Geophys. Res.*, 112, D02201, doi:10.1029/2006JD007547, 2007.

944 Boers, R., Acarreta, J. A., and Gras, J. L.: Satellite monitoring of the first indirect aerosol effect: Retrieval of
945 the droplet concentration of water clouds, *J. Geophys. Res.*, 111, D22208, doi:10.1029/2005JD006838,
946 2006.

947 Boucher, O., and Quaas, J.: Water vapour affects both rain and aerosol optical depth, *Nat. Geosci.*, 6, 4-5,
948 doi:10.1038/ngeo1692, 2012.

949 Chen, Q., Yin, Y., Jin, L., Xiao, H., and Zhu, S.: The effect of aerosol layers on convective cloud
950 microphysics and precipitation, *Atmos. Res.*, 101, 327-340, doi:10.1016/j.atmosres.2011.03.007, 2011.

951 Cheng, C. T., Wang, W. C., and Chen, J. P.: A modeling study of aerosol impacts on cloud microphysics and
952 radiative properties, *Q. J. R. Meteorol. Soc.*, 133, 283-297, doi:10.1002/qj.25, 2007.

953 Cheng, C. T., Wang, W. C., and Chen, J. P.: Simulation of the effects of increasing cloud condensation nuclei
954 on mixed-phase clouds and precipitation of a front system, *Atmos. Res.*, 96, 461-476, doi:
955 10.1016/j.atmosres.2010.02.005, 2010.

956 Chylek, P., Dubey, M. K., Lohmann, U., Ramanathan, V., Kaufman, Y. J., Lesins, G., Hudson, J., Altmann,
957 G., and Olsen, S.: Aerosol indirect effect over the Indian Ocean, *Geophys. Res. Lett.*, 33, L06806,
958 doi:10.1029/2005GL025397, 2006.

959 Dee, D. P., Uppala, S. M., Simmons, A. J., Berrisford, P., Poli, P., Kobayashi, S., Andrae, U., Balmaseda, M.
960 A., Balsamo, G., Bauer, P., Bechtold, P., Beljaars, A. C. M., van de Berg, L., Bidlot, J., Bormann, N.,
961 Delsol, C., Dragani, R., Fuentes, M., Geer, A. J., Haimberger, L., Healy, S. B., Hersbach, H., Hólm, E.
962 V., Isaksen, I., Kållberg, P., Köhler, M., Matricardi, M., McNally, A. P., Monge-Sanz, B. M.,
963 Morcrette, J.-J., Park, B.-K., Peubey, C., de Rosnay, P., Tavolato, C., Thépaut, J.-N., Vitart, F.: The
964 ERA-Interim reanalysis: configuration and performance of the data assimilation system, *Q. J. R.*
965 *Meteorol. Soc.*, 137, 553-597, doi:10.1002/qj.828, 2011.

966 Fan, J. W., Rosenfeld, D., Yang, Y., Zhao, C., Leung, L. R., and Li, Z. Q.: Substantial contribution of
967 anthropogenic air pollution to catastrophic floods in Southwest China, *Geophys. Res. Lett.*, 42,
968 6066-6075, doi:10.1002/2015GL064479, 2015.

969 Garrett, T. J. and Zhao, C.: Increased Arctic cloud longwave emissivity associated with pollution from
970 mid-latitudes, *Nature*, 440, 787-789, doi:10.1038/nature04636, 2006.

971 Givati, A., and Rosenfeld, D.: Quantifying precipitation suppression due to air pollution, *J. Appl. Meteor.*, 43,
972 1038-1056, doi:10.1175/1520-0450(2004)043<1038:QPSDTA>2.0.CO;2, 2004.

973 Grandey, B. S., and Stier, P.: A critical look at spatial scale choices in satellite-based aerosol indirect effect
974 studies, *Atmos. Chem. Phys.*, 10, 11459-11470, doi:10.5194/acp-10-11459-2010, 2010.

975 Grandey, B. S., Stier, P. and Wagner, T. M.: Investigating relationships between aerosol optical depth and
976 cloud fraction using satellite, aerosol reanalysis and general circulation model data, *Atmos. Chem. Phys.*,
977 13, 3177-3184, doi:10.5194/acp-13-3177-2013, 2013.

978 Gryspeerdt, E., Sourdeval, O., Quaas, J., Delanoë, J., Krämer, M., and Kühne, P.: Ice crystal number
979 concentration estimates from lidar–radar satellite remote sensing – Part 2: Controls on the ice crystal
980 number concentration, *Atmos. Chem. Phys.*, 18, 14351–14370, doi:10.5194/acp-18-14351-2018, 2018.

981 Gryspeerdt, E., Stier, P., and Grandey, B. S.: Cloud fraction mediates the aerosol optical depth-cloud top
982 height relationship, *Geophys. Res. Lett.*, 41, 3622-3627, doi:10.1002/2014GL059524, 2014a.

983 Gryspeerdt, E., Stier, P., and Partridge, D. G.: Links between satellite-retrieved aerosol and precipitation,
984 *Atmos. Chem. Phys.*, 14, 9677–9694, doi:10.5194/acp-14-9677-2014, 2014b.

985 Gunthe, S. S., Rose, D., Su, H., Garland, R. M., Achtert, P., Nowak, A., Wiedensohler, A., Kuwata, M.,
986 Takegawa, N., Kondo, Y., Hu, M., Shao, M., Zhu, T., Andreae, M. O., and Poschl, U.: Cloud
987 condensation nuclei (CCN) from fresh and aged air pollution in the megacity region of Beijing, *Atmos.*
988 *Chem. Phys.*, 11, 11023-11039, doi:10.5194/acp-11-11023-2011, 2011.

989 Guo, C. W., Xiao, H., Yang, H. L., and Tang, Q.: Observation and modeling analyses of the macro-and
990 microphysical characteristics of a heavy rain storm in Beijing, *Atmos. Res.*, 156, 125-141,
991 doi:10.1016/j.atmosres.2015.01.007, 2015.

992 Guo, J. P., Deng, M. J., Lee, S. S., Wang, F., Li, Z. Q., Zhai, P. M., Liu, H., Lv, W., Yao, W., and Li, X. W.:
993 Delaying precipitation and lightning by air pollution over the Pearl River Delta, Part I: Observational
994 analyses. *J. Geophys. Res.*, 121, 6472-6488, doi:10.1002/2015JD023257, 2016.

995 Guo, L., Highwood, E. J., Shaffrey, L. C., and Turner, A. G.: The effect of regional changes in anthropogenic
996 aerosols on rainfall of the East Asian Summer Monsoon, *Atmos. Chem. Phys.*, 13, 1521-1534,
997 doi:10.5194/acp-13-1521-2013, 2013.

998 Guo, X. L., Fu, D. H., Guo, X., and Zhang, C. M.: A case study of aerosol impacts on summer convective
999 clouds and precipitation over northern China, *Atmos. Res.*, 142, 142-157,
1000 doi:10.1016/j.atmosres.2013.10.006, 2014.

1001 Hammer, M. S., Martin, R. V., Li, C., Torres, O., Manning, M., and Boys, B. L.: Insight into global trends in
1002 aerosol composition from 2005 to 2015 inferred from the OMI Ultraviolet Aerosol Index, *Atmos. Chem.*
1003 *Phys.*, 18, 8097-8112, doi:10.5194/acp-18-8097-2018, 2018.

1004 Harikishan, G., Padmakumari, B., Mahes Kumar, R. S., Pandithurai, G., and Min, Q. L.: Aerosol indirect effects
1005 from ground-based retrievals over the rain shadow region in Indian subcontinent, *J. Geophys. Res.*, 121,
1006 2369-2382, doi:10.1002/2015JD024577, 2016.

1007 Higgins, R. W., Yao, Y., Yarosh, E. S., Janowiak, J. E. and Mo, K. C.: Influence of the Great Plains low-level
1008 jet on summertime precipitation and moisture transport over the central United States, *J. Climate*, 10,
1009 481-507, doi:10.1175/1520-0442(1997)010<0481:IOTGPL>2.0.CO;2, 1997.

1010 Holz, R. E., Ackerman, S. A., Nagle, F. W., Frey, R., Dutcher, S., Kuehn, R. E., Vaughan, M. A., and Baum,

.011 B.: Global Moderate Resolution Imaging Spectroradiometer (MODIS) cloud detection and height
.012 evaluation using CALIOP, *J. Geophys. Res.*, 113, D00A19, doi: 10.1029/2008JD009837, 2008.

.013 Jacobson, M. Z.: Strong radiative heating due to the mixing state of black carbon in atmospheric aerosols,
.014 *Nature*, 409, 695-697, doi:10.1038/35055518, 2001.

.015 Jiang, H., Feingold, G., and Cotton, W. R.: Simulations of aerosol-cloud-dynamical feedbacks resulting from
.016 entrainment of aerosol into the marine boundary layer during the Atlantic Stratocumulus Transition
.017 Experiment, *J. Geophys. Res.*, 107(D24), 4813, doi:10.1029/2001JD001502, 2002.

.018 Jiang, J. H., Su, H., Schoeberl, M. R., Massie, S. T., Colarco, P., Platnick, S., and Livesey, N. J.: Clean and
.019 polluted clouds: Relationships among pollution, ice clouds, and precipitation in South America, *Geophys.*
.020 *Res. Lett.*, 35, L14804, doi: 10.1029/2008GL034631, 2008.

.021 Jiang, M. J., Li, Z. Q., Wan, B. C., and Cribb, M.: Impact of aerosols on precipitation from deep convective
.022 clouds in eastern China, *J. Geophys. Res.*, 121, 9607-9620, doi:10.1002/2015JD024246, 2016.

.023 Johnson, D. B.: The role of giant and ultra-giant aerosol particles in warm rain initiation, *J. Atmos. Sci.*, 39,
.024 448-460, doi:10.1175/1520-0469(1982)039<0448:TROGAU>2.0.CO;2, 1982.

.025 Jung, W. S., Panicker, A. S., Lee, D. I., and Park, S. H.: Estimates of aerosol indirect effect from Terra
.026 MODIS over Republic of Korea, *Advances in Meteorology*, 2013 (976813), 1-8,
.027 doi:10.1155/2013/976813, 2013.

.028 Kim, K. -M., Lau, K. M., Sud, Y. C., and Walker, G. K.: Influence of aerosol radiative forcings on the diurnal
.029 and seasonal cycles of rainfall over West Africa and Eastern Atlantic Ocean using GCM simulation, *Clim.*
.030 *Dyn.*, 35, 115-126, doi: 10.1007/s00382-010-0750-1, 2010.

.031 Lau, K. M., Kim, M. K., and Kim, K. M.: Asian summer monsoon anomalies induced by aerosol direct
.032 forcing: the role of the Tibetan Plateau, *Clim. Dyn.*, 26, 855-864, doi:10.1007/s00382-006-0114-z, 2006.

.033 Lee, S. S., Donner, L. J., and Phillips, V. T. J.: Impacts of aerosol chemical composition on microphysics and
.034 precipitation in deep convection, *Atmos. Res.*, 94, 220-237, doi:10.1016/j.atmosres.2009.05.015, 2009.

.035 Lee, S. S., Guo, J., and Li, Z.: Delaying precipitation by air pollution over the Pearl River Delta: 2. Model
.036 simulation, *J. Geophys. Res.*, 121, 11739-11760, doi:10.1002/2015JD024362, 2016.

.037 Lelieveld, J. and Heintzenberg, J.: Sulfate cooling effect on climate through in-cloud oxidation of
.038 anthropogenic SO₂, *Science*, 258, 117-120, doi:10.1126/science.258.5079.117, 1992.

.039 Levy, R. C., Mattoo, S., Munchak, L. A., Remer, L. A., Sayer, A. M., Patadia, F., and Hsu, N. C.: The
.040 Collection 6 MODIS aerosol products over land and ocean, *Atmos. Meas. Tech.*, 6, 2989-3034,
.041 doi:10.5194/amt-6-2989-2013, 2013.

.042 Li, H., Cui, X., Zhang, W., and Qiao, L.: Observational and dynamic downscaling analysis of a heavy rainfall
.043 event in Beijing, China during the 2008 Olympic Games, *Atmos. Sci. Lett.*, 17, 368-376,
.044 doi:10.1002/asl.667, 2016.

.045 Li, Z., Niu, F., Fan, J., Liu, Y., Rosenfeld, D., and Ding, Y.: Long-term impacts of aerosols on the vertical
.046 development of clouds and precipitation, *Nat. Geosci.*, 4, 888-894, doi:10.1038/ngeo1313, 2011.

.047 Lim, K. S. and Hong, S.: Investigation of aerosol indirect effects on simulated flash-flood heavy rainfall over
.048 Korea, *Meteor. Atmos. Phys.*, 118, 199-214, doi:10.1007/s00703-012-0216-6, 2012.

.049 Liu, G., Shao, H., Coakley Jr. J. A., Curry, J. A., Haggerty, J. A., and Tschudi, M. A.: Retrieval of cloud
.050 droplet size from visible and microwave radiometric measurements during INDOEX: Implication to
.051 aerosols' indirect radioactive effect, *J. Geophys. Res.*, 108(D1), 4006, doi:10.1029/2001JD001395, 2003.

.052 Liu, J., Wang, S., Zhang, W., and Wei, X.: Mechanism analysis of a strong convective weather in Hebei
.053 Province, *Advances in Marine Science*, 30, 9-16, 2012. (in Chinese)

.054 Menzel, W. P., Frey, R. A., Zhang, H., Wylie, D. P., Moeller, C. C., Holz, R. E., Maddux, B., Baum, B. A.,
.055 Strabala, K. I., and Gumley, L. E.: MODIS global cloud-top pressure and amount estimation: Algorithm
.056 description and results, *J. Appl. Meteorol. Clim.*, 47, 1175-1198, doi: 10.1175/2007JAMC1705.1, 2008.

.057 Min, Q., Joseph, E., Lin, Y., Min, L., Yin, B., Daum, P. H., Kleinman, L. I., Wang, J., and Lee, Y. -N.:
.058 Comparison of MODIS cloud microphysical properties with in-situ measurements over the Southeast
.059 Pacific, *Atmos. Chem. Phys.*, 12, 11261-11273, doi:10.5194/acp-12-11261-2012, 2012.

.060 Nakajima, T. and King, M. D.: Determination of the optical thickness and effective particle radius of clouds
.061 from reflected solar radiation measurements. Part I: Theory, *J. Atmos. Sci.*, 47, 1878-1893,
.062 doi:10.1175/1520-0469(1990)047<1878:DOTOTA>2.0.CO;2, 1990.

.063 Panicker, A. S., Pandithurai, G., and Dipu, S.: Aerosol indirect effect during successive contrasting monsoon
.064 seasons over Indian subcontinent using MODIS data, *Atmos. Environ.*, 44, 1937-1943,
.065 doi:10.1016/j.atmosenv.2010.02.015, 2010.

.066 Platnick, S., Meyer, K., King, M. D., Wind, G., Amarasinghe, N., Marchant, B., Arnold, G. T., Zhang, Z.,
.067 Hubanks, P. A., Holz, R. E., Yang, P., Ridgway, W. L., and Riedi, J.: The MODIS cloud optical and
.068 microphysical products: Collection 6 updates and examples from Terra and Aqua, *IEEE Trans. Geosci.*
.069 *Remote Sens.*, 55, 502-525, doi:10.1109/TGRS.2016.2610522, 2017.

.070 Qian, Y., Gong, D. Y., Fan, J. W., Leung, L. R., Bennartz, R., Chen, D. L., Wang, W. G.: Heavy pollution
.071 suppresses light rain in China: Observations and modeling, *J. Geophys. Res.*, 114, D00K02,
.072 doi:10.1029/2008JD011575, 2009.

.073 Qiu, Y., Zhao, C., Guo, J., and Li, J.: 8-Year ground-based observational analysis about the seasonal variation
.074 of the aerosol-cloud droplet effective radius relationship at SGP site, *Atmos. Environ.*, 164, 139-146,
.075 doi:10.1016/j.atmosenv.2017.06.002, 2017.

.076 Quaas, J., Boucher, O., Bellouin, N. and Kinne, S.: Satellite-based estimate of the direct and indirect aerosol
.077 climate forcing, *J. Geophys. Res.*, 113, D05204, doi:10.1029/2007JD008962, 2008.

.078 Quaas, J., Stevens, B., Stier, P., and Lohmann U.: Interpreting the cloud cover aerosol optical depth
.079 relationship found in satellite data using a general circulation model, *Atmos. Chem. Phys.*, 10, 6129-6135,
.080 doi:10.5194/acp-10-6129-2010, 2010.

.081 Reutter, P., Su, H., Trentmann, J., Simmel, M., Rose, D., Gunthe, S. S., Wernli, H., Andreae, M. O., and
.082 Po ¨schl, U.: Aerosol- and updraft-limited regimes of cloud droplet formation: influence of particle

.083 number, size and hygroscopicity on the activation of cloud condensation nuclei (CCN), *Atmos. Chem.*
.084 *Phys.*, 9, 7067-7080, doi:10.5194/acp-9-7067-2009, 2009.

.085 Rienecker, M. M., Suarez, M. J., Todling, R., Bacmeister, J., Takacs, L., Liu, H. C., Gu, W., Sienkiewicz, M.,
.086 Koster, R. D., Gelaro, R., Stajner, I., Nielsen, J. E.: The GEOS-5 Data Assimilation
.087 System—Documentation of Versions 5.0.1 and 5.1.0, and 5.2.0. NASA Technical Report Series on
.088 Global Modeling and Data Assimilation NASA/TM-2008 -104606 27: 92 pp, 2008.

.089 Rosenfeld, D.: TRMM observed first direct evidence of smoke from forest fires inhibiting rainfall, *Geophys.*
.090 *Res. Lett.*, 26, 3105–3108, doi:10.1029/1999GL006066, 1999.

.091 Rosenfeld, D., Lohmann, U., Raga, G. B., O'Dowd, C. D., Kulmala, M., Fuzzi, S., Reissell, A., Andreae, M.
.092 O.: Flood or drought: How do aerosols affect precipitation? *Science*, 321, 1309-1313,
.093 doi:10.1126/science.1160606, 2008.

.094 Rosenfeld, D., Sherwood, S., Wood, R., and Donner, L.: Climate effects of aerosol-cloud interactions, *Science*,
.095 343, 379-380, doi:10.1126/science.1247490, 2014.

.096 Rosenfeld, D., and Woodley, W. L.: Convective clouds with sustained highly supercooled liquid water down
.097 to -37.5°C, *Nature*, 405, 440–442, doi:10.1038/35013030, 2000.

.098 Sassen, K., Starr, D., Mace, G. G., Poellot, M. R., Melfi, S. H., Eberhard, W.L., Spinhirne, J. D., Eloranta, E.
.099 W., Hagan, D. E., and Hallett, J.: The 5–6 December 1991 FIRE IFO II jet stream cirrus case study:
.100 Possible influences of volcanic aerosols, *J. Atmos. Sci.*, 52, 97–123, doi:10.1175/1520-0469(1995)
.101 052<0097:TDFIJJ>2.0.CO;2, 1995.

.102 Shen, Y., Xiong, A., Wang, Y., and Xie, P.: Performance of high-resolution satellite precipitation products
.103 over China, *J. Geophys. Res.*, 115, D02114, doi:10.1029/2009JD012097, 2010.

.104 Sherwood, S.: Aerosols and ice particle size in tropical cumulonimbus, *J. Clim.*, 15, 1051–1063,
.105 doi:10.1175/1520-0442(2002)015<1051:AAIPSI>2.0.CO;2, 2002.

.106 Shinzuka, Y., Clarke, A. D., Nenes, A., Jefferson, A., Wood, R., McNaughton, C. S., Ström, J., Tunved, P.,
.107 Redemann, J., Thornhill, K. L., Moore, R. H., Latham, T. L., Lin, J. J., and Yoon, Y. J.: The relationship
.108 between cloud condensation nuclei (CCN) concentration and light extinction of dried particles:
.109 indications of underlying aerosol processes and implications for satellite-based CCN estimates, *Atmos.*
.110 *Chem. Phys.*, 15, 7585-7604, doi:10.5194/acp-15-7585-2015, 2015.

.111 Song, X. L. and Zhang, G. J.: Microphysics parameterization for connective clouds in a global climate model:
.112 Description and single-column model tests, *J. Geophys. Res.*, 116, D02201, doi:10.1029/2010JD014833,
.113 2011.

.114 Squires, P.: The growth of cloud drops by condensation: I. general characteristics, *Aust. J. Sci. Res., Ser. A*, 5,
.115 66–86, 1952.

.116 Squires, P., and Twomey, S.: A comparison of cloud nucleus measurements over central North America and
.117 Caribbean Sea, *J. Atmos. Sci.*, 23, 401–404, doi: 10.1175/1520-0469(1966)023<0401:ACOCNM>
.118 -2.0.CO;2, 1966.

.119 Sun, Y. L., Wang, Z. F., Du, W., Zhang, Q., Wang, Q. Q., Fu, P. Q., Pan, X. L., Li, J., Jayne, J., and Worsnop,
.120 D. R.: Long-term real-time measurements of aerosol particle composition in Beijing, China: seasonal
.121 variations, meteorological effects, and source analysis, *Atmos. Chem. Phys.*, 15, 10149-10165,
.122 doi:10.5194/acp-15-10149-2015, 2015.

.123 Tariq, S., and Ali, M.: Spatio-temporal distribution of absorbing aerosols over Pakistan retrieved from OMI on
.124 board Aura Satellite, *Atmos. Pollution Res.*, doi: 10.5094/APR.2015.030, 2015.

.125 Tao, M. H., Chen, L. F., Wang, Z. F., Tao, J. H., Che, H. Z., Wang, X. H., and Wang, Y.: Comparison and
.126 evaluation of the MODIS Collection 6 aerosol data in China, *J. Geophys. Res.*, 120, 6992-7005,
.127 doi:10.1002/2015JD023360, 2015.

.128 Tao, W. K., Chen, J. P., Li, Z., Wang, C., and Zhang C.: Impact of aerosols on convective clouds and
.129 precipitation, *Rev. Geophys.*, 50, RG2001/2012, 1-62, doi: 10.1029/2011RG000369, 2012.

.130 Torres, O., Bhartia, P.K., Herman, J.R., Ahmad, Z., Gleason, J.: Derivation of aerosol properties from satellite
.131 measurements of backscattered ultraviolet radiation: Theoretical basis, *J. Geophys. Res.*, 103, 17099–
.132 17110, doi:10.1029/98JD00900, 1998.

.133 Twohy, C. H., Coakley, J. A., and Tahnk, W. R.: Effect of changes in relative humidity on aerosol scattering
.134 near clouds, *J. Geophys. Res.*, 114, D05205, doi:10.1029/2008JD010991, 2009.

.135 Twomey, S.: The influence of pollution on the shortwave albedo of clouds, *J. Atmos. Sci.*, 34, 1149–1152,
.136 doi:10.1175/1520-0469(1977)034<1149:TIOPO>2.0.CO;2, 1977.

.137 Wang, J., Feng, J., Wu, Q., and Z. Yan, Z.: Impact of anthropogenic aerosols on summer precipitation in the
.138 Beijing-Tianjin-Hebei urban agglomeration in China: Regional climate modeling using WRF-Chem, *Adv.*
.139 *Atmos. Sci.*, 33, 753-766, doi:10.1007/s00376-015-5103-x, 2016.

.140 Wolyn, P. G., and Mckee, T. B.: The mountain plains circulation east of a 2-km-high north south barrier, *Mon.*
.141 *Weather Rev.*, 122, 1490-1508, doi:10.1175/1520-0493(1994)122<1490:TMPCEO>2.0.CO;2, 1994.

.142 Wu, P., Ding, Y. H., and Liu, Y. J.: Atmospheric circulation and dynamic mechanism for persistent haze
.143 events in the Beijing-Tianjin-Hebei region, *Adv. Atmos. Sci.*, 34, 429-440,
.144 doi:10.1007/s00376-016-6158-z, 2017.

.145 Yang, X., Zhao, C., Zhou, L., Li, Z., Cribb, M., and Yang, S.: Wintertime cooling and a potential connection
.146 with transported aerosols in Hong Kong during recent decades, *Atmos. Res.*, 211, 52-61,
.147 doi:10.1016/j.atmosres.2018.04.029, 2018.

.148 Yu, R. C., Zhou, T. J., Xiong, A. Y., Zhu, Y. J., and Li, J. M.: Diurnal variations of summer precipitation over
.149 contiguous China, *Geophys. Res. Lett.*, 34, L017041, doi:10.1029/2006GL028129, 2007.

.150 Yuan, T., Li, Z., Zhang, R., and Fan, J.: Increase of cloud droplet size with aerosol optical depth: An
.151 observation and modeling study, *J. Geophys. Res.*, 113, D04201, doi:10.1029/2007JD008632, 2008.

.152 Yuan, W. H., Yu, R. C., Chen, H. M., Li, J., and Zhang, M. H.: Subseasonal Characteristics of Diurnal
.153 Variation in Summer Monsoon Rainfall over Central Eastern China, *J. Climate*, 23, 6684-6695,
.154 doi:10.1175/2010JCLI3805.1, 2010.

.155 Zeng, S., Riedi, J., Trepte, C. R., Winker, D. M., and Hu, Y. -X.: Study of global cloud droplet number
.156 concentration with A-Train satellites, *Atmos. Chem. Phys.*, 14, 7125-7134, doi:
.157 10.5194/acp-14-7125-2014, 2014.

.158 Zhao, B., Gu, Y., Liou, K. -N., Wang, Y., Liu, X., Huang, L., Jiang, J. H., and Su, H.: Type-Dependent
.159 Responses of Ice Cloud Properties to Aerosols From Satellite Retrievals, *Geophys. Res. Lett.*, 45, 3297–
.160 3306, doi:10.1002/2018GL077261, 2018.

.161 Zhou, S., Yang, J., Wang, W. C., Gong, D., Shi, P., and Gao, M.: Shift of daily rainfall peaks over the
.162 Beijing–Tianjin–Hebei region: An indication of pollutant effects? *Int. J. Climatol.* 2018;1–10,
.163 doi:10.1002/joc.5700, 2018.

.164 Zhu, Y., Rosenfeld, D., and Li, Z.: Under what conditions can we trust retrieved cloud drop concentrations in
.165 broken marine stratocumulus? *J. Geophys. Res.*, 123, 8754-8767, doi:10.1029/2017JD028083, 2018.

.167 **Tables**

.168

Indicator	Source	Begin time	Thresholds	
			25 th percentile	75 th percentile
AOD	MODIS	2002	0.98	2.00
CDNC (cm ⁻³)	MODIS	2002	80.70	199.08
AAI	OMI	2005	0.13	0.52
SAI	OMI	2005	- 0.13	- 0.35
AOD of BC	MACC	2003	0.04	0.06
AOD of sulfate	MACC	2003	0.46	0.87
SH at 850 hPa (g/kg)	ERA-interim	2002	9.96	12.95

.169

.170 Table 1. The indicators of aerosols and moisture used in the study and their sources, begin times and the
.171 thresholds (25th and 75th percentiles). The end time of all data is to 2012.

.172

.173

.174

.175

Siyuan 20/2/19 11:34 PM

Indicator	Soi
AOD	MC
CDNC (cm ⁻³)	MC
AAI	O
SAI	O
AOD of BC	M/
AOD of sulfate	M/
SH at 850 hPa (g/kg)	ERA-

已删除:

Characteristics of heavy rainfall	Clean		Polluted		Difference		Significance	
	AOD	CDNC	AOD	CDNC	AOD	CDNC	AOD	CDNC
Start time	24.2 (3.9)	22.4 (4.3)	23.5 (4.8)	20.2 (4.1)	- 0.7	- 2.2	P<0.05	P<0.05
Peak time	23.0 (4.0)	22.2 (5.7)	22.0 (4.8)	19.6 (5.4)	- 1.0	- 2.6	P<0.05	P<0.05
Duration	4.0 (2.1)	5.9 (3.7)	4.8 (2.8)	6.4 (3.9)	0.8	0.5	P<0.05	P<0.05
Intensity	164.9 (98.4)	166.4 (92.4)	169.6 (94.3)	163.2 (90.0)	4.7	- 3.2	P>0.1	P>0.1

Siyuan 20/2/19 11:34 PM

Characteristics of heavy rainfall	Clean	
	AOD	CDNC
Start time	24.2 (3.9)	
Peak time	23.0 (4.0)	
Duration	4.0 (2.1)	
Intensity	164.9 (98.4)	

已删除:

Table 2. The mean values of start time (units: LST), peak time (units: LST), duration (units: hours) and intensity (units: 0.1mm/hour) of heavy rainfall respectively on the clean and polluted conditions using two indicators of AOD and CDNC, and their differences (polluted minus clean) and significances. The numbers in the brackets stand for the standard deviations on the means. "P<0.05" stands for the difference has passed the significance test of 95%, and "P>0.1" stands for the difference did not pass the significance test of 90%.

Characteristics of heavy rainfall	AAI	SAI	Difference (AAI-SAI)	Less BC	More BC	Difference (More-Less)	Less sulfate	More sulfate	Difference (More-Less)
Start time	23.4 (4.8)	24.1 (4.4)	-0.7	24.2 (4.8)	23.9 (4.4)	-0.3	24.0 (4.3)	24.5 (4.4)	0.5
Peak time	21.0 (5.3)	22.6 (5.1)	-1.6	23.4 (5.3)	22.3 (4.0)	-1.1	23.2 (4.5)	22.9 (4.8)	-0.3
Duration	5.0 (3.1)	6.0 (3.8)	-1.0	4.8 (2.6)	4.6 (2.7)	-0.2	4.0 (2.1)	5.5 (3.0)	1.5

Table 3. The mean values of start time (units: LST), peak time (units: LST) and duration (units: hours) of heavy rainfall respectively on the conditions with more absorbing aerosols (AAI more than 75th percentile, from OMI), more scattering aerosols (SAI more than 75th percentile, from OMI), less or more BC (AOD of BC less than 25th or more than 75th percentile, from MACC), less or more sulfate (AOD of sulfate less than 25th or more than 75th percentile, from MACC), and their differences. Numbers in the brackets stand for the standard deviations on the means. All differences have passed the significant test of 95%.

Clean/Polluted	CF	CTP	COT		CWP		CER		
			liquid	ice	liquid	ice	liquid	ice	
AOD	Clean	62.8 (17.6)	442.3 (149.6)	6.9 (4.5)	6.7 (8.5)	62.8 (36.6)	123.1 (168.9)	16.7 (4.4)	32.0 (8.7)
	Polluted	89.3 (12.9)	487.3 (145.7)	10.0 (5.8)	12.9 (17.0)	96.4 (52.5)	211.3 (279.3)	17.5 (3.5)	29.2 (9.0)
CDNC	Clean	95.4 (5.7)	369.9 (110.0)	11.7 (12.9)	8.7 (13.6)	153.2 (159.0)	238.0 (281.9)	20.0 (2.8)	34.1 (5.5)
	Polluted	96.9 (4.7)	460.1 (145.6)	28.4 (22.3)	33.1 (22.6)	265.6 (210.4)	462.1 (443.5)	12.5 (2.0)	24.6 (8.9)

Siyuan 20/2/19 11:34 PM

Clean/Polluted	CF
AOD	Clean 62.8 (17.6)
	Polluted 89.3 (12.9)
CDNC	Clean 94.5 (6.1)
	Polluted 97.4 (4.2)

已删除:

.197
.198 Table 4. The mean values of CF (units: %), CTP (units: hPa), COT (liquid and ice, units: none), CWP (liquid
.199 and ice, units: g/m^3) and CER (liquid and ice, units: μm) from MODIS C6 cloud product on the clean
.200 condition (less than 25th percentile) and polluted condition (more than 75th percentile) using two indicators of
.201 AOD and CDNC. Numbers in the brackets stand for the standard deviations on the means. Numbers in grey
.202 indicate the results of liquid COT & CER are related to the calculation of CDNC. The differences between
.203 clean and polluted conditions have all passed the significant test of 95%.
.204
.205
.206
.207

Group (case number)	CF	CTP	COT		CWP		CER	
			liquid	ice	liquid	ice	liquid	ice
1.Clean, dry (123)	91.7 (6.8)	413.5 (129.4)	9.9 (9.0)	7.9 (8.9)	119.9 (122.7)	163.2 (180.9)	19.9 (2.8)	35.7 (6.2)
2.Polluted, dry (140)	96.0 (4.9)	493.6 (140.1)	39.2 (24.6)	37.3 (22.4)	311.0 (233.3)	683.5 (458.0)	12.5 (2.1)	28.3 (8.2)
3.Clean, wet (178)	95.6 (6.0)	464.3 (131.1)	19.2 (17.9)	18.0 (17.9)	219.4 (216.5)	354.9 (364.3)	<i>19.2 (2.7)</i> <i>$p_{1,3}>0.05$</i>	32.7 (4.3)
4.Polluted, wet (195)	97.5 (4.7)	<i>462.7 (156.4)</i> <i>$p_{3,4}>0.05$</i>	32.2 (22.0)	24.6 (21.4)	259.0 (219.1)	393.3 (418.3)	12.8 (2.1)	24.0 (8.2)

Siyuan 20/2/19 11:34 PM

Group (case number)	CF
1 Clean, dry (153)	93.8 (6.1)
2 Polluted, dry (128)	95.6 (5.1)
3 Clean, wet (155)	<i>92.7 (7.0)</i> <i>$p_{1,3}>0.05$</i>
4 Polluted, wet (194)	97.8 (4.4)

已删除:

.208
.209 Table 5. The mean values of CF (units: %), CTP (units: hPa), COT (liquid and ice, units: none), CWP (liquid
.210 and ice, units: g/m^3) and CER (liquid and ice, units: μm) in four groups. Numbers in the brackets stand for the
.211 standard deviations on the means. Italic numbers in grey represent that the differences are not significant, in
.212 which “ $P>0.05$ ” stands for the difference did not pass the significance test of 95%.
.213
.214
.215

Siyuan 20/2/19 11:34 PM

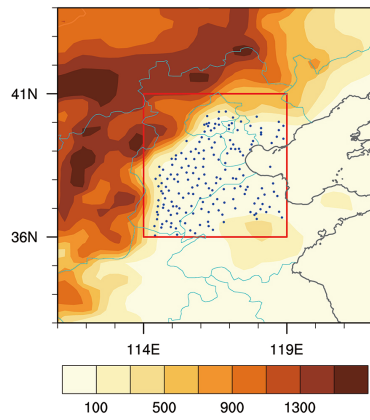
已删除: has passed the significance test of 90% but

Siyuan 20/2/19 11:34 PM

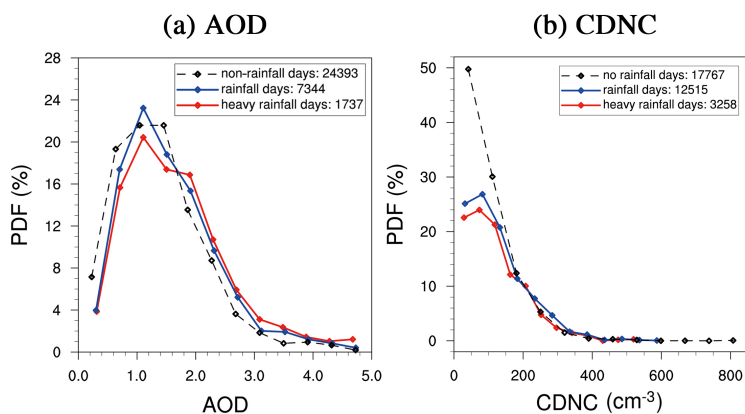
已删除: %, and “ $P>0.1$ ” stands for the difference did not pass the significance test of 90

.223
.224
.225
.226
.227
.228
.229
.230
.231
.232
.233
.234
.235
.236
.237
.238
.239
.240
.241
.242
.243

Figures



.244
.245 Figure 1. Selected rainfall stations (blue dots) and topography (shading, units: m) in the BTH region (red box,
.246 36–41° N, 114–119° E).
.247



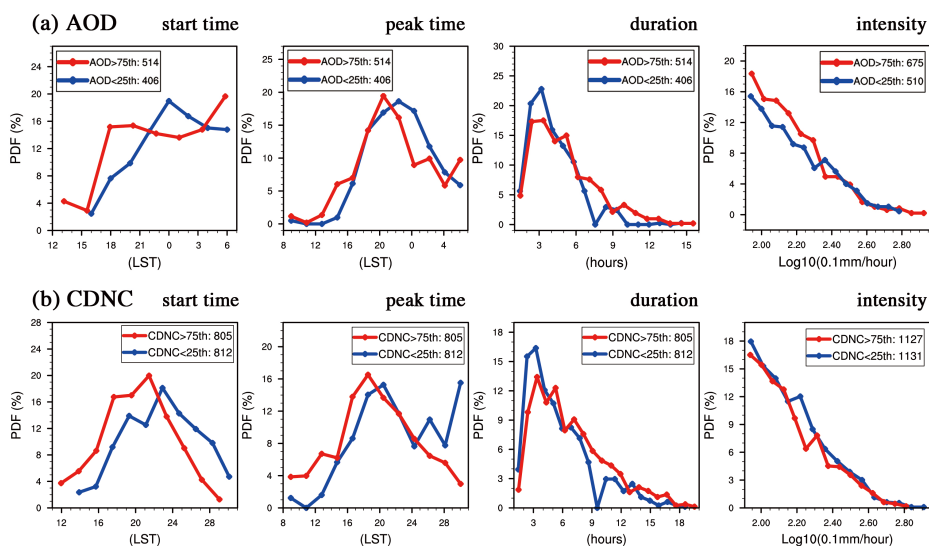
249

250 Figure 2. PDF of (a) AOD and (b) CDNC (cm^{-3}) (data from MODIS) on non-rainfall days (black lines),
 251 rainfall days (blue lines) and heavy rainfall days (red lines) in southwesterly during early summers from 2002
 252 to 2012. Numbers in the legends denote the sample number.

253

254

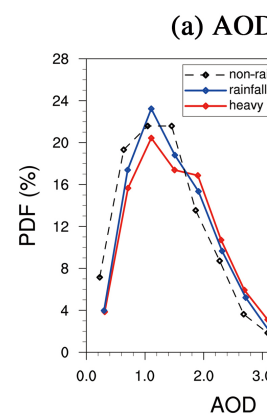
255



256

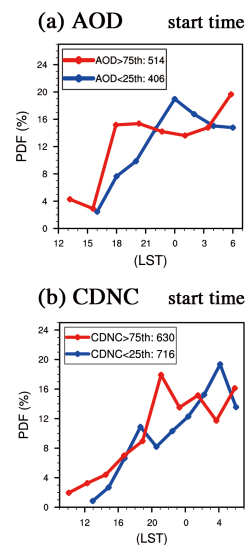
257 Figure 3. PDF of start time (units: LST), peak time (units: LST), duration (units: hours) and intensity (units:

Siyuan 20/2/19 11:34 PM



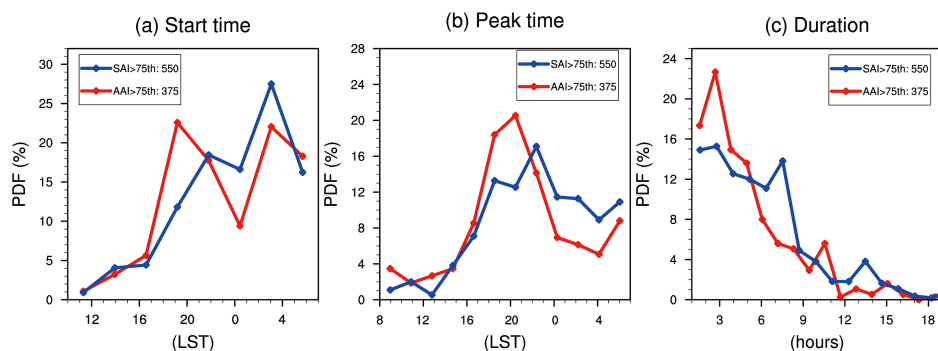
已删除:

Siyuan 20/2/19 11:34 PM

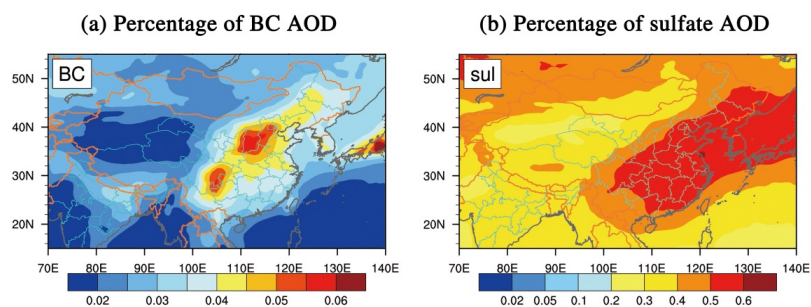


已删除:

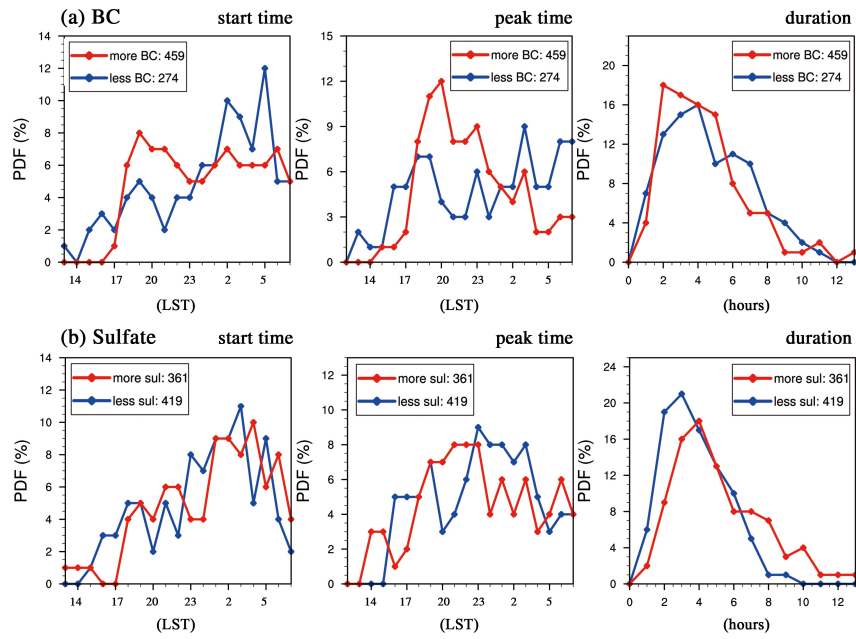
.260 0.1mm/hour) of heavy rainfall (data from CMA) on selected clean (blue lines) and polluted (red lines)
 .261 conditions, respectively using indicator of (a) AOD and (b) CDNC (cm^{-3}), during early summers from 2002 to
 .262 2012.
 .263



.264
 .265 Figure 4. PDF of (a) start time (units: LST), (b) peak time (units: LST), and (c) duration (units: hours) of
 .266 heavy rainfall on the days with SAI more than 75th percentile (blue lines, data from OMI) and days with AAI
 .267 more than 75th percentile (red lines, data from OMI), during early summers from 2005 to 2012.
 .268
 .269



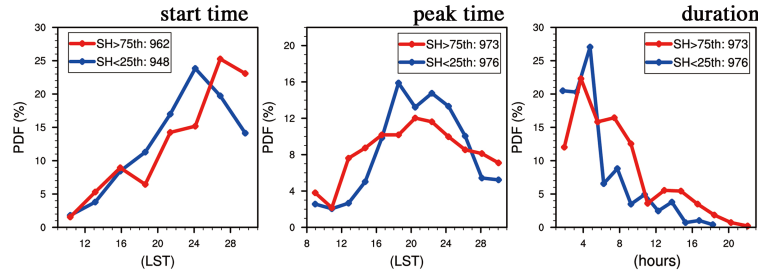
.270
 .271 Figure 5. Percentages of AOD for (a) BC and (b) sulfate from MACC reanalysis data in summers (June –
 .272 August) during 2002 to 2012.
 .273
 .274
 .275



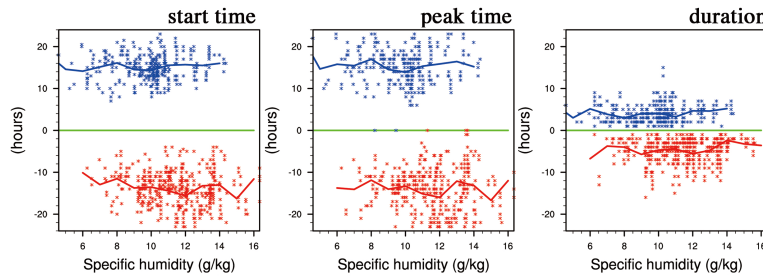
.276
.277 Figure 6. PDF of start time (units: LST), peak time (units: LST) and duration (units: hours) of heavy rainfall
.278 on the different conditions of (a) BC and (b) sulfate. Blue/red lines stand for the condition of less/more BC or
.279 sulfate (AOD of BC or sulfate less than 25th /more than 75th percentile, data from MACC) during early
.280 summers from 2003 to 2012.

.281
.282

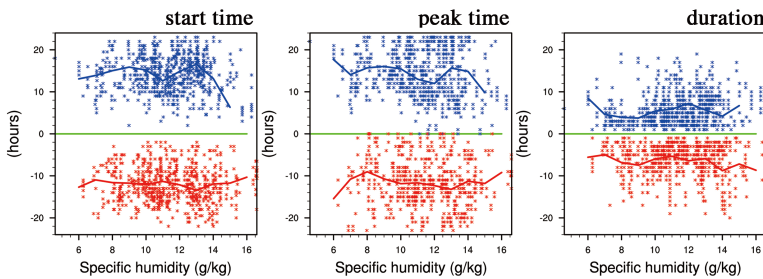
(a) PDF with more/less SH



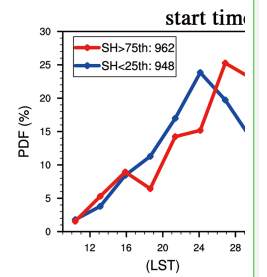
(b) Scatter distribution using AOD



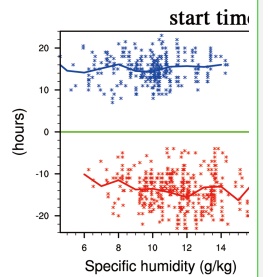
(c) Scatter distribution using CDNC



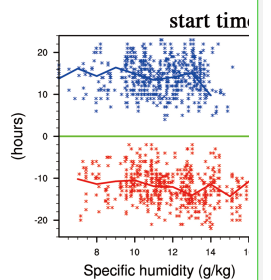
(a) PDF with more/less SH



(b) Scatter distribution using AOD



(c) Scatter distribution using CDNC



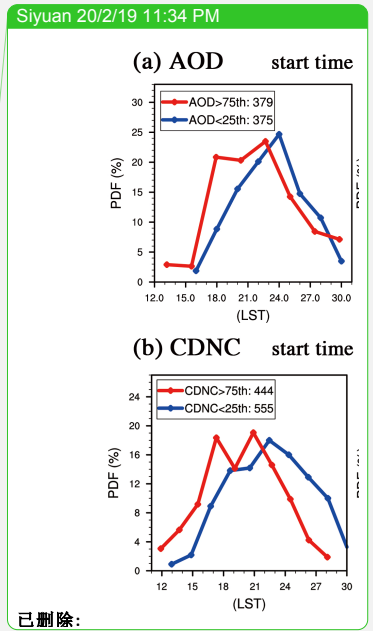
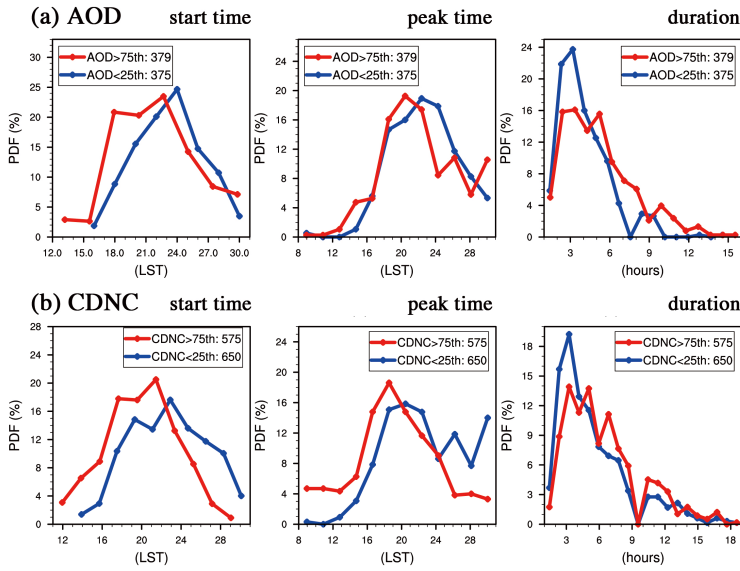
已删除:

.283

.284 Figure 7. (a) PDF of start time (units: LST), peak time (units: LST), and duration (units: hours) of heavy
.285 rainfall with less moisture (blue lines, SH at 850 hPa less than 25th percentile, data form ERA-interim) and
.286 more moisture (red lines, SH at 850 hPa more than 75th percentile, data form ERA-interim). (b) and (c) are
.287 scatter distributions of SH-start time/peak time/duration for clean cases (blue points) and polluted cases (red
.288 points) respectively using AOD and CDNC. Green lines stands for the start/peak time at 8:00 LST or the
.289 duration is 0 hours. Positive (negative) values stand for the hours away from 8:00 LST or 0 hours in clean
.290 (polluted) cases. Blue (red) lines stand for the mean values of rainfall characteristics at each integer of SH in
.291 clean (polluted) cases.

.292

.293



.295

.296

.297 Figure 8. PDF of start time (units: LST), peak time (units: LST), and duration (units: hours) of heavy rainfall
.298 on selected clean (blue lines) and polluted (red lines) conditions with SH at 850 hPa (from ERA-interim) less
.299 than 75th percentile, respectively using indicator of (a) AOD and (b) CDNC (cm^{-3}), during early summers from
.300 2002 to 2012.

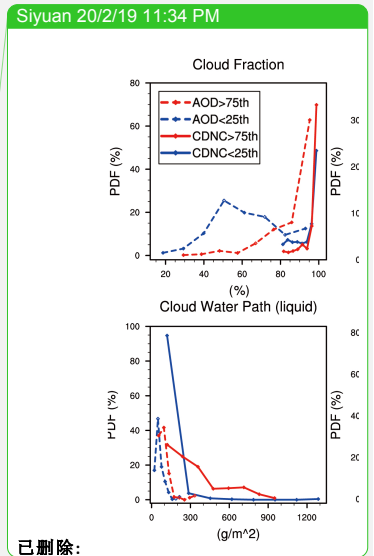
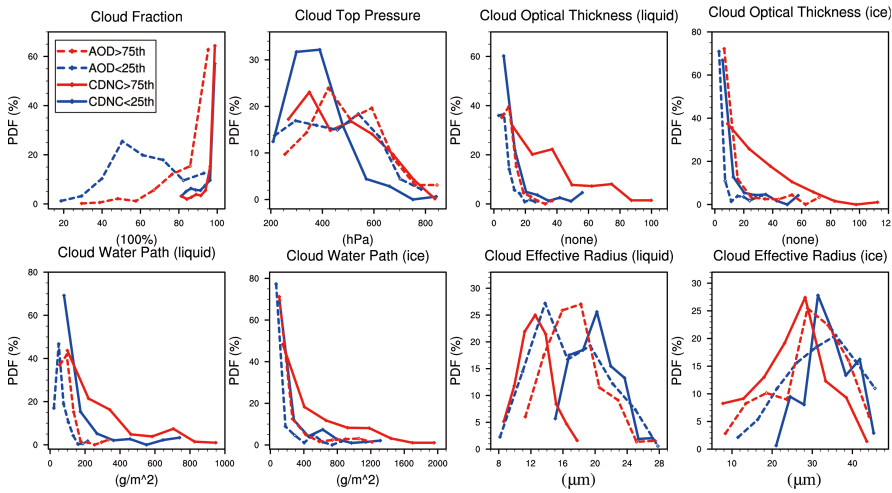
.301

.302

.303

.304

.305



.307

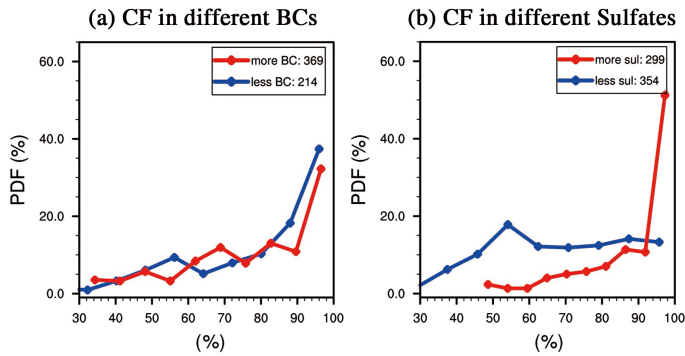
.308 Figure 9. PDF of CF (units: %), CTP (units: hPa), COT (liquid and ice, units: none), CWP (liquid and ice,
.309 units: g/m^2) and CER (liquid and ice, units: μm) on selected clean (blue dash lines: AOD<25th percentile; blue
.310 solid lines: CDNC<25th percentile) and polluted (red dash lines: AOD>75th percentile; red solid lines:
.311 CDNC>75th percentile) heavy rainfall days. All cloud variables are obtained from MODIS C6 cloud product.

.312

.313

.314

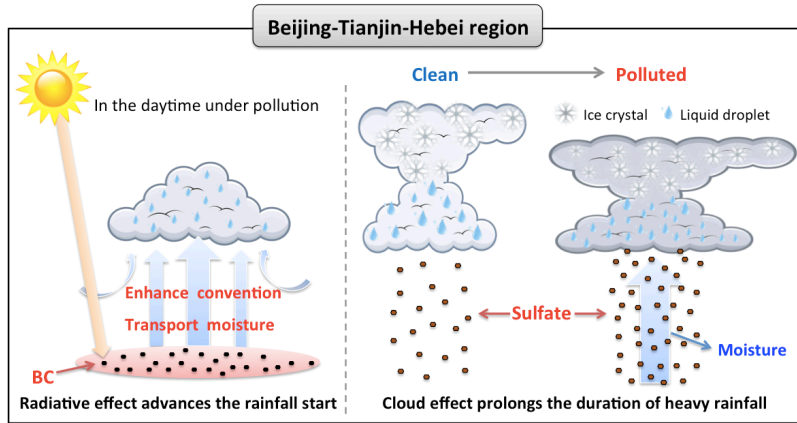
.315



.316

.317 Figure 10. PDF of CF (units: %, data from MODIS) respectively for the conditions of less BC/sulfate (blue
.318 lines, AOD of BC/sulfate less than 25th percentile, data from MACC) and more BC/sulfate (red lines, AOD of
.319 BC/sulfate more than 75th percentile, data from MACC) cases with heavy rainfall during 10 early summers
.320 (2003-2012).

.322
.323
.324



.325
.326
.327
.328
.329

Figure 11. A schematic diagram for aerosol impacts on heavy rainfall over Beijing-Tianjin-Hebei region.